This is a repository copy of *A litho-tectonic event stratigraphy from dynamic Late Devensian ice flow of the North Sea Lobe, Tunstall, east Yorkshire, UK*.

White Rose Research Online URL for this paper:
https://eprints.whiterose.ac.uk/160745/

Version: Accepted Version

A litho-tectonic event stratigraphy from dynamic Late Devensian ice flow of the North Sea Lobe, Tunstall, east Yorkshire, UK

Jenna L. Sutherland[1, 2*], Bethan J. Davies[1], Jonathan R. Lee[3]

[1]Department of Geography, Royal Holloway University of London, Egham, Surrey, TW20 OEX, United Kingdom

[2]School of Geography, University of Leeds, Woodhouse Lane, Leeds, West Yorkshire, LS2 9JT, United Kingdom

[3]British Geological Survey, Keyworth, Nottingham, NG12 5GG, United Kingdom

*Correspondence to:

Jenna Sutherland

Email: gyjls@leeds.ac.uk

Tel.: 0113 343 3324

ABSTRACT

The central sector of the British-Irish Ice Sheet during the last glaciation was characterised by complex ice-flow reflecting interacting ice streams and changing dominance of different ice dispersal centres. At Tunstall, east Yorkshire, two subglacial till units have been traditionally identified as the Late Devensian Skipsea and Withernsea tills, and thought to record two separate ice advances onto the Holderness coast, from divergent ice flow directions. Our study presents the first quantitative lithological, sedimentological and structural evaluation of glacial sediments at the site. The lithological composition of both till units suggests that ice extended southwards from southern Scotland, incorporating material from north-east England and the western margin of the North Sea Basin. Notably, the bulk lithological properties of both the Skipsea and Withernsea tills are very similar. Subtle variations in colour, texture and lithology that do occur simply appear to reflect spatial and temporal variability in subglacial entrainment along the flow path of the North Sea Lobe. The relative arrangements of the units plus the fracture sets also indicates phases of intra-till thrust-stacking and unloading (F2), consolidation and shrinkage (F1, F3) suggestive of cycles of ice re-advance (thrusting) and ice-marginal retreat (unloading and shrinkage) possibly relating to active recession. The findings from this study reveal a sedimentary and structural complexity that is not recognised by the current Late Devensian till stratigraphy of east Yorkshire.

38

39 **1. INTRODUCTION**

40 Palaeo-ice sheets are important analogues for understanding contemporary ice sheets,

41 offering a record of ice sheet behaviour that can span millennia (Ely *et al*., 2019). The last

42 British-Irish Ice Sheet (BIIS) provides an excellent analogue for understanding the character

43 and behaviour of modern marine-based ice sheets due to its comparatively small size,

44 accessible bed, and the wealth of pre-existing information (e.g. Evans *et al*., 2005;

45 Livingstone *et al*., 2012; McMillan and Merritt, 2012; Clark *et al*., 2012; 2018).

46 Approximately two thirds of the BIIS was marine-based, drained by ice streams and fringed

47 by ice shelves in many places (Clark *et al*., 2012; Gandy *et al*., 2018, 2019), making it a

48 good analogue for the West Antarctic Ice Sheet (WAIS; Hubbard *et al*., 2009). This is

49 especially so because the BIIS deglaciated in response to rising temperatures and a rising

50 sea level (driven by melting of other ice masses), which are the current forces that might

51 cause collapse of the WAIS (Bamber *et al*., 2009; DeConto and Pollard, 2016).

52 Reconstructing the behaviour of palaeo-ice sheets enables a better understanding of the

53 long-term (centennial to millennial) behaviour of ice sheets within the Earth system. Only

54 when the mechanisms from palaeo-ice sheets, such as the BIIS, are better constrained, can

55 such knowledge be used for improving the next generation of numerical ice sheet models

56 used in sea-level forecasting (Stokes *et al*., 2015; Ely *et al*., 2019).

57 The body of empirical evidence related to the BIIS has progressively developed over the last

58 decade in particular (e.g. Clark *et al*., 2012, 2018; Hughes *et al*., 2016; Small *et al*., 2017;

Bateman *et al*., 2018; Bradwell *et al*., 2019; Davies *et al*., 2019; Ely *et al*., 2019; Lovell *et al*., 2019), producing an ever-expanding database of palaeo-ice sheet data, but there are still gaps in knowledge regarding ice-marginal processes (Roberts *et al*., 2013) and their implications for glacier dynamics. Eastern England and the North Sea Basin are the main areas of complexity and uncertainty due to multiple competing ice lobes and potential ice flow reversals (Evans *et al*., 2019). The ice limits, interactions between ice lobes, and their relative chronologies in this area are only broadly known and, without this understanding, the glaciodynamic history and the nature of the BIIS remains contested.

In order to address outstanding questions on the character and behaviour of part of the southeast sector of the last BIIS, this study has three main aims. Firstly, this study will determine the depositional processes and a relative event stratigraphy for the Late Devensian sediments observed at Tunstall, eastern England (**Figure 1**). Secondly, this study will determine the provenance of the glaciogenic sequence in order to reconstruct the glacial transport pathway for the deposits. Thirdly, this study will integrate this event stratigraphy and sediment provenance information into the broader Late Devensian evolution of the region and southeast sector of the last BIIS.

2. STUDY AREA AND PREVIOUS INVESTIGATIONS

A southward advance of the North Sea Lobe (NSL) of the last BIIS during the Late Devensian (Weichselian; Dimlington Stadial; MIS 2) resulted in the development of till sequences across parts of County Durham, east Yorkshire, Lincolnshire and north Norfolk (Pawley *et al*., 2006; Catt, 2007; Davies *et al*., 2009, 2013; Boston *et al*., 2010; Evans and Thomson, 2010; Bateman *et al*., 2011, 2015, 2017; Roberts *et al*., 2013). The glacial lithostratigraphy of the Holderness coast, east Yorkshire (**Figure 1B**), has traditionally been

83   subdivided into three till units (the Basement Till, Skipsea Till, and Withernsea Till

84   respectively), based principally upon particle size distribution, sediment colour, clast

85   lithology, heavy mineral composition and matrix calcium carbonate content (Madgett and

86   Catt, 1978; Catt, 2007). Optically Stimulated Luminescence (OSL) ages constrain the timing

87   of initial advance of the NSL into the region, and deposition of the Skipsea Till, to ~21.7 ka

88   (**Figure 1**), reaching its maximum extent at ~19.5 ka (Evans *et al*., 2019) with offshore

89   retreat occurring at ~18 ka (Bateman *et al*., 2011, 2015, 2017). The recession of the NSL

90   was initially rapid followed by a series of near synchronous oscillations of the NSL, and

91   subsequent deposition of the Withernsea Till at ~16.8 ka, before the final terminal retreat of

92   the ice sheet occurring prior to ~15.5 ka (Bateman *et al*., 2017).

93   Catt (2007) described the Skipsea Till as possessing a dark-greyish brown (10YR 3/2)

94   colour and occupying the whole Holderness area. The Skipsea Till is correlative with the

95   Late Devensian Horden Till Formation in County Durham (Davies *et al*., 2009; 2012), based

96   on stratigraphic relationships and sedimentary petrography. According to Pawley *et al*.

97   (2008), on the basis of correlative luminescence dates, the north Norfolk equivalent of the

98   Skipsea Till is the Holkham (Hunstanton) Till. However, recent OSL dating has suggested a

99   slightly earlier incursion of ice into north Norfolk timed at ~21.5 ka (Evans *et al*., 2019).

100   Bisat (1939) and Radge (1939), suggested that the Skipsea Till was deposited by ice flowing

101   into Eastern England through the Stainmore Gap from the Lake District and Pennines, while

102   the Withernsea Till originated from the Cheviots and Southern Uplands. Later studies

103   documented a suite of erratics derived from Scotland, Northumberland, and the Cheviots

104   (Catt and Penny, 1966; Madgett and Catt, 1978; Catt, 2007). Busfield *et al*. (2015)

105   confirmed, from quantitative clast data and derived microfossils, that the Skipsea Till was

106   sourced from southern Scotland, incorporating material from north eastern England,

107   northeast Yorkshire and the western margin of the North Sea Basin.

108   The overlying Withernsea Till (dark-reddish brown, 5 YR 3/4 in its weathered form) by

109   contrast is less widespread, cropping-out in south east Holderness (**Figure 1C**) (Evans and

110   Thomson, 2010). North of Flamborough Head, the Withernsea Till reappears as the Upper

111   Till Series of Edwards (1981, 1987), seen in coastal cliffs of Filey Bay. However, Bisat

112   (1939) suggested that the till is confined to isolated basins within this area. The Withernsea

113   Till can be less confidently provenanced to its source area although erratics recorded

114   suggest a source from the Lake District and Pennines (Catt and Penny, 1966; Catt and

115   Digby, 1988; Bell and Forster, 1991). The red colouration is also strongly suggestive of

116   input of Permo-Triassic materials from the Sherwood Sandstone and/or Mercia Mudstone

117   groups. The fragmented, crenulated ridges developed within the landscape of Holderness

118   (**Figure 1C**; Evans *et al*., 2001; Evans and Thomson, 2010; Clark *et al*., 2018) and

119   superimposed upon the Skipsea and Withernsea Tills have been interpreted as lateral

120   moraines and also suggest an ice-flow direction from the north and east.

121   Using geochemical data from samples at seven sites along the Holderness coast, Boston *et*

122   *al*. (2010) argued that the Basement, Skipsea and Withernsea Tills could not be statistically

123   differentiated, with more variation within than between the tills. This raised significant

124   questions regarding the stratigraphical correlation of Late Devensian tills in east Yorkshire

125   and Lincolnshire. Boston *et al*. (2010) concluded that the till units are not lithologically

126   distinct and that the current stratigraphy does not recognise the sedimentary and structural

127   complexity produced by repeated onshore, possibly surging flow by a dynamic NSL along

128   the eastern margin of the BIIS (based on stacked sequences; Evans and Thomson, 2010).

129   Clast lithology has been used effectively to quantify ice-flow pathways and provenance for

130   the Skipsea Till (Busfield *et al*., 2015), but no comparative work has yet been undertaken

131   for the Withernsea Till.

132   With some of the most rapidly eroding coastline in northern Europe (Bird, 2010; Castedo *et*

133   *al.*, 2015), the Holderness coast provides an ideal opportunity to assess extensive cliff

134   exposures through the Quaternary geology. Tunstall is centrally located within the limits of

135   both the Skipsea and Withernsea tills (**Figure 1C**), offering a valuable opportunity for a

136   comparative study between the two tills deposited in superposition. Excluding a

137   comprehensive soil profile examination by Madgett and Catt (1978) (**Figure 1D**), there has

138   been little previously published process or provenance work conducted at Tunstall. Due to

139   this lack of quantitative and detailed analysis, the understanding of till genesis remains

140   underdeveloped. The site at Tunstall, therefore, offers an excellent opportunity to use

141   detailed clast lithological analysis and detailed process-based sedimentology to untangle the

142   stratigraphic relationships, ice-flow pathways and provenance of the Skipsea and

143   Withernsea Tills.

144

145   ### 3. METHODS

146   We present new quantitative sedimentological investigations of the Late Devensian till

147   sequence that crops-out above Cretaceous chalk bedrock at Tunstall, east Yorkshire (**Figure**

148   **1D**), together with a comprehensive clast lithological provenance analysis critical to the

149   palaeoglaciological reconstruction of the eastern sector of the BIIS.

150   Eight exposures were logged in detail from 2 km of vertical coastal cliff sections at Tunstall,

151   east Yorkshire (0°0'6.9"E, 53°45'24.7"N). At each site, vertical profile logs were compiled

152   from cleared sections. Following procedures outlined in Evans and Benn (2004), the

153   sedimentary characteristics were recorded including unit thickness, modal grain size,

154   sedimentary and tectonic structures, degree of consolidation, matrix *vs* clast supported

155   nature, grading and sorting of each unit, Munsell colour, bed geometry, and the nature of

6

contacts between the units. Sediments were described using standard facies codes (following

Benn and Evans, 1998) and reclassified into lithofacies associations (LFAs) to aid regional

correlation. In order to convey the lateral changes in architecture and localised complexity

in structural features, detailed field sketches and cross sections, supported by photographic

evidence, were utilised to accurately map the geometry of the exposures and create an

overall facies architecture map.

A three-order clast morphological analysis was used, encompassing clast shape,

angularity/roundness and stone orientation to help establish the depositional history of the

sediment (cf. Evans and Benn, 2004; Hubbard and Glasser, 2005; Hambrey and Glasser,

2012). Where possible, palaeo-current measurements were taken on stratified deposits. Clast

fabrics, striae measurements and eigenvector analyses followed Benn (1994) and Hubbard

and Glasser (2005). The structural data is presented in equal area stereographic projections

as poles to planes. Bulk samples for particle size analysis (PSA) and clast lithological

analysis (CLA) were collected from a 2 m^2 area in each lithofacies to give a statistically

significant, representative sample (Bridgland, 1986). The minimum sample size was 201

clasts; however, >300 clasts were counted in 4 of the 8 samples. At least two replicate

samples from each lithofacies for both PSA and CLA were taken to ensure the heterogeneity

within the stratigraphy was accounted for. Due to the spatial variability and clast-poor

nature of the diamicton units, bulk samples of at least 10 kg were collected. PSA was

undertaken in order to describe the textural properties of the sediments and support genetic

interpretation (Gale and Hoare, 2012). PSA was conducted using a laser granulometer for

particles <2000 µm and dry sieving for particles >2000 µm. The lithology of all recovered

clasts in the 8-16 mm, 16-32 mm, and >32 mm size fractions was identified using a low-

powered binocular microscope and compared to a reference collection and standard rock

180   identification criteria (Evans and Benn, 2004, Walden, 2004, Stow, 2005; Gale and Hoare,

181   2012).

182   Multivariate statistical analysis was performed on the clast lithological data using Principal

183   Component Analysis (PCA). PCA is commonly used in both regional geochemical and

184   lithostratigraphical studies (Gibbard, 1985; 1986; Cheshire, 1986; Scheib *et al*., 2011). The

185   data are easily reduced into a smaller number of interrelated groups that reveal underlying

186   patterns or 'principal components' within lithological datasets. PCA axes simplify and

187   represent variation in the data (Davis, 1986) to identify key variables, and relationships

188   between variables, within a dataset (Richards, 1998; Lee, 2003; Davies *et al*., 2009). The

189   analysis was run using the covariance matrix method (Kovach, 1995) which is strongly

190   affected by non-normally distributed data and outliers (Reimann *et al*., 2008). Like other

191   exploratory multivariate statistical techniques, PCA provides eigenvectors, or 'principal

192   component coefficients' to describe the relative significance of individual (lithological)

193   components and their variability within the data set. Associated eigenvalues or 'principal

194   component scores' record the percentage of the total variance of each principal component,

195   in this case, measuring the importance of each lithology relative to each other in describing

196   the characteristics of a particular sample.

197

198   **4.   RESULTS: SITE SEDIMENTOLOGY AND STRATIGRAPHY**

199   *4.1 Facies Architecture*

200   The stratigraphic architecture of the exposures at Tunstall is summarised in **Figure 2**.

201   Vertical profile logs 1 - 8 (**Figure 3a, b**) reveal four distinct Lithofacies Associations

202   (LFAs). Bedrock is not exposed and the LFAs identified vary both vertically and laterally.

203   The summarised relative stratigraphic succession observed in the field is as follows; dark

coloured diamict (LFA 1) exposed towards the north of the section, overlain by red-coloured

diamict (LFA 2), which is in-turn overlain by clast-supported sands and gravels with a

sharp, unconformable, undulating base (LFA 3). A distinctly white organic silt (LFA 4)

crops-out intermittently for a short distance within the LFA 3 succession in the middle of

the lateral section. Above LFA 4 is a thin unit of LFA 3b and the top of the sequence is

capped by a thin soil horizon ~10 cm thick.

The surface of the cliff undulates, and the middle section has been heavily human-modified.

The height of the section varies between 4 m at the lowest point, where there is a break in

the cliffs for beach access, to ~12 m at the highest. Slumping along the length of the section

is widespread due to the instability of the cliffs obscuring many of the *in-situ* sediments. An

unusual feature of the section at Tunstall is the numerous natural cliff promontories that

protrude out ~ 3m towards the sea. Coastal erosion is non-uniform and some spurs are more

prominent than others. An even distance of 10 - 15 m separates the spurs from each other

along the beach.

4.2 Lithofacies Descriptions

LFA 1

LFA 1 is a dark brown (7.5 YR 3/4), matrix-supported, massive and homogenised diamicton

with a dense clay-matrix texture, containing clasts ranging from fine gravels to small

boulders up to 25 cm in diameter (**Table 1**). It has an over-consolidated nature. The

thickness of LFA 1 varies between 0 - 6 m and is exposed only in the northernmost part of

the section (**Figure 2**; **Figure 3b**; Section logs 5 to 8). The majority of clasts within LFA 1

are sub-angular (34 %) to sub-rounded (38 %) (**Figure 6B**), incorporating a high proportion

of facetted and striated clasts (**Figure 6E**). The overall clast morphology is dominated by

'blocky' shapes (**Figure 6C**). The diamicton contains numerous laterally-extensive thin (<5

228 cm) lenses of gravel that dip 30 º to the south and can be traced along the section in several

229 places (**Figure 3b**; Section logs 7 and 8). It possesses a generally weak clast fabric at each

230 locality sampled (**Figure 2**); with a polymodal distribution of points but clustering towards

231 the southeast. Stringers also occur in the lower few metres of the unit, just above the beach

232 level, persisting up to 1 m before pinching out. LFA 1 is fissile, observed particularly at the

233 boundary between LFA 1 and LFA 2. The upper contact with LFA 2 is sharp with a concave

234 base. The base of the LFA 1 was obscured by the beach.

235 *LFA 2*

236 LFA 2 is a massive, matrix-supported, bright reddish brown (5 YR 5/6) sandy diamicton

237 (**Table 1**). LFA 2 is consistently exposed to the south of the section where the cliffs are ~11

238 m high (**Figure 2**). The average clast morphology of LFA 2 is 'blocky' (**Figure 6C**) with a

239 high proportion of facetted (31%) and striated (6%) clasts (**Figure 6E**). Larger boulders and

240 cobbles are observed at variable heights and orientations and are heavily striated with often

241 more than one striae orientation (**Figure 2**). The clast fabric is weak, with a polymodal

242 distribution of points but a fairly weak clustering from the northwest to the southeast

243 (**Figure 2**). The striae measurements show a clearer directional indicator, towards the south-

244 west, than the clast fabrics (**Figure 2**). The majority of clasts are sub-angular to rounded

245 (**Figure 6B**). LFA 2 is largely massive at the macroscale, but stringers also occur as

246 numerous streaks of red and black diamicton up to 10 cm thick (**Figure 4b**). Discontinuous

247 lateral beds (~30 cm) of grey diamicton alternate between thicker units (>50 cm) of the

248 brown diamicton (**Figure 4d, e**) with sharp contacts above and below the interbeds. Thin,

249 dipping sand and gravel laminations towards the northeast are observed at variable heights

250 within LFA 2. In Section log 5 (**Figure 3b**), cross-bedded gravelly sands were observed in

251 LFA 2 and a gravel pod that pinches laterally. The gravel pod is composed of laminated fine

252 sands and fine gravels that coarsen-upwards.

253   *LFA 3*

254 LFA 3 is best illustrated in Section Logs 1, 2, 4, 7, and 8 (**Figure 3a, b**). LFA 3 is laterally

255 variable, observed intermittently every few meters along the length of the exposure, often

256 capping the sequence just below the soil horizon. Overall, there are three lithofacies present

257 within LFA 3; planar laminated dark clays and silts (LF 3a), planar, cross-bedded fine sands

258 (LF 3b), and cobbles and gravels (LF 3c). The basal contact of LFA 3 is undulating, with

259 elevations ranging from 1.2 m to 8 m. It is repeatedly down-cut into the underlying

260 diamicton (LFA 1 or 2) in a concave-shaped depression and has a sharp, erosive base (e.g.

261 **Figure 3a**; Section log 1). The upper contact with either LFA 4 or the soil horizon is planar

262 and sharp.

263 LF 3a is dominated by horizontal laminated dark clays and silts, which coarsen upwards into

264 massive fine sands (LF 3b). Thin (<5 cm) laterally-continuous seams of coal fragments and

265 particles (mm – cm) occur within the sandy unit of LF 3b. LF 3c consists of well-sorted,

266 well-rounded, clast-supported coarse pebbles and cobbles (**Table 1**) that are stratified and

267 imbricated towards the northwest (**Figure 3a;** Section Log 4**; Figure 4g, h**). Randomly

268 orientated, clast-supported, coarse gravels of LF 3c typically infill the concave structures

269 (**Figure 4g**) and numerous pebble lags are observed along the bases of the channel-like

270 structures. The majority of clasts are well-rounded (28 %), rounded (32 %) and sub-rounded

271 (24 %), with only 4 % faceted and no clasts striated (**Figure 6B**, **C**, **E**). Up to 14 % of the

272 stones are broken. The unit thickness of LF 3c is typically thicker than LF 3a and b.

273   *LFA 4*

274 LFA 4 is laterally discontinuous and only crops-out within LFA 3 near the surface of the

275 southernmost part of the section (**Figure 4f**). LFA 4 comprises a bright white (7.5YR 8/1)

276 silt which highly calcareous (57 % calcium carbonate content). The contacts above and

277 below LFA 4 are very sharp and linear. The unit of the lower boundary has a slight elliptical

278 shape covering a discontinuous lateral extent of roughly 300 m. The deposit is uniformly 20

279 cm thick and is densely packed with small shells deposited in their life position. The

280 majority of the shells within the sediment are freshwater gastropods including abundant

281 *Radix bulthica*, *Lymnaea peregra*, and *Galba truncatula*, but other freshwater snails

282 *Planorbis viviparis*, *Valvata crisata* and aquatic bivalves of *Pisidium* genus are also present.

283   *4.3 Lithofacies interpretations*

284   *LFA 1 and 2*

285 LFA 1 and LFA 2 possess many bulk characteristics of a subglacial traction till such as their

286 matrix-supported texture, highly fissile, and over-consolidated nature, in addition to the

287 presence of faceted and striated lithologies of wide-ranging provenance (cf. Evans *et al*.,

288 2006). A subglacial traction till is defined by Evans *et al*. (2006) to include sediments that

289 accreted by sliding over and/or deforming at the glacier bed, sediment released directly from

290 the ice by pressure melting, and sediment completely or largely homogenised by shearing.

291 The fissile structures, observed at the boundary between the tills are interpreted here to be

292 very small, thin thrust faults. Clast rotation within subglacial traction tills results in shape

293 alignment of elongate, low-sphericity grains such as those observed in LFA 1 and 2 (**Figure**

294 **6B, C**). Where clasts have been brought into contact while lodged on a rigid bed and

295 moving in the subglacial traction zone, they typically have bullet-shaped and faceted ends

296 (Boulton and Hindmarsh, 1987; Kruger, 1979, 1984, 1994; Sharp, 1982), such as those in

297 LFA 1 and 2 (**Figure 6E**). Other structures within both lithofacies indicative of lodgement,

298 such as their massive homogenised appearance, occur in association with structures

299 indicative of subglacial deformation, including stringer initiation and deformed inclusions of

300 LFA 1 in LFA 2 (**Figure 4b**, **d**, **e**), as well as weak clast macrofabrics (**Figure 2; Figure 3a,**

301 **b**); Evans *et al*., 1995; Hicock and Fuller, 1995, Hart 1997; Bennett *et al*., 1999; Roberts and

302   Hart, 2005). Stringers of red and black diamicton (particularly in LFA 2) are, therefore,

303   interpreted as tectonic laminae produced by the progressive shearing and attenuation of soft

304   sediment inclusions (Hart and Roberts, 1994; Phillips *et al*., 2008). Most of these structures

305   indicate that the till was formed under low strain conditions with elevated porewater

306   pressures (van der Wateren, 1995; Hiemstra *et al*., 2007; Lee and Phillips, 2008); however,

307   strain rates can vary both spatially and temporally as pore-water pressure fluctuates, creating

308   a mosaic of deformation (Piotrowski *et al*., 2004; Lee and Phillips, 2008; Lee, 2009). This

309   may explain why some of the sections at Tunstall, particularly of LFA 1, are more massive

310   and are completely homogenised than others, while delicate deformation structures, such as

311   stringers, are preserved elsewhere.

312   *LFA 3*

313   Overall, a glaciofluvial origin is suggested for LFA 3 based upon the coarse-grained

314   characteristics of LF 3c in addition to the evidence for abrupt discharge fluctuations,

315   recorded in discontinuous, lensate bodies of cross-bedded sands (LF 3b) which are likely to

316   be post-glacial winnowed lags. These packages of massive to crudely horizontally-bedded

317   sheets, separated by lower discharge scour infills, are typical of strongly episodic fluvial

318   sedimentation, classified as gravel sheets by Miall (1977) and Maizels (1993). The

319   horizontally-bedded glaciofluvial outwash assemblage records rapidly fluctuating

320   discharges, as evidenced by abrupt vertical changes from boulder gravels to the laminated

321   sediments typical of overbank fines or waning discharge drapes (Miall, 1977, 1985;

322   Collinson, 1996).

323   The irregular, concave base of the LFA 3 basal contact is interpreted as an erosional base

324   with concave-up bases and flat tops (**Figure 4g**) permitting isolated channelized forms that

325   have been shaped by the erosive force of water incising into the underlying sediments. The

326   gravel facies that infill the isolated channel forms, in addition to the strong variation in

327 height of these channels, support the interpretation of deposition in a proximal setting for

328 LFA 3, interpreted as the product of high energy proglacial outwash when the ice was

329 retreating (Miall, 1977; Maizels, 1995). Due to the lack of large-scale trough cross-bedding

330 and the cyclic fining-upwards sequence of gravels, sands and silts, distal proglacial outwash

331 sedimentation has been excluded as a mechanism for the deposition of LFA 3. Instead, LF

332 3a could have been deposited by under-melt at the ice-bed interface in subglacial canals (cf.

333 Walder and Fowler, 1994), perhaps indicative of ice-bed decoupling and sliding, or in Nye

334 channels, similar to those that have been observed elsewhere in Devensian sediments in

335 Northeast England (Eyles *et al*., 1982; Davies *et al*., 2009). The pebble lags evident in LFA

336 3a point to evidence of bedload saltation, whereby pebbles have been rolled along in

337 flowing water at the boundary of the bed and formed a lag.

338 The direction of the imbricated clasts of LF 3c indicates a palaeo-flow direction from the

339 northeast. The majority of clasts in LFA 3c are rounded (**Figure 4b; Figure 6B**) which

340 indicates highly abrasive high energy conditions in a fast-flowing current, whereas the

341 lenses of bedded sands, and stratified gravels are indicative of moderate flow regimes with

342 frequent changes in flow regime and sediment supply. An increasing energy regime is also

343 implied by the upwards coarsening of the sequence. Changes in the dominance of flow

344 suggest the presence of fast, hyperconcentrated flows, as well as slower moving, lower

345 energy flows.

346 *LFA 4*

347 The freshwater gastropods *Radix bulthica*, *Radix peregra*, *Galba truncatula*, *Panorbis*

348 *viviparous* and *Valvata cristata* all inhabit the same type of environment; stagnant or slow

349 moving water (Kerney *et al*., 1980). Due to the abundance of these freshwater gastropods,

350 the depositional environment is inferred to be a spring-fed vegetated calcareous pool or

351 shallow film of water trickling across wet ground such as a Tufa (Garnett *et al*., 2004). Tufa

352 is a variety of limestone formed by the precipitation of carbonate minerals from ambient

353 temperature water bodies and forms either in fluvial channels or lacustrine settings. The

354 deposit at Tunstall is likely to have occurred from an emergence of a spring or seep, due to

355 its thin bed thickness and discontinuous lateral extent. Spring-fed paludal deposits are

356 widespread on or near limestone bedrock (Andrews *et al*., 2000).

357   *4.4 Structural genesis*

358   *Fracture description*

359 A series of horizontal and vertical fractures dissect the lower sections of the cliffs at

360 Tunstall. In places, these fractures have been eroded and enlarged by wave action. Overall,

361 four distinct fracture sets are observed within the cliff exposures; three sub-vertical sets (F1,

362 F3 and F4), punctuated by a sub-horizontal fracture set (F2). Given their continuous

363 presence and abundance along the cliff exposure, the fractures are inherent structural

364 features of the deposits at Tunstall.

365 The F1 fracture set occurs discontinuously at the base of the cliffs within LFA 1 material.

366 They are vertical to sub-vertical fractures, up to 1.5 m in length, that strike broadly

367 northeast-southwest and variably dip towards the northwest and southeast at angles >75 °

368 (**Figure 5**). The density of the fractures is spatially variable, being more densely

369 concentrated at the base of each cliff promontory but occurring along the entire length of the

370 described section (**Figure 4a**, **c**, **d, i**). The density of fractures varies with zones of high

371 density (spacing ranging from 1 - 20 cm) and low density (spacing range from 20 - 100 cm)

372 fracturing. The F1 fracture set extends up to, and is truncated by, a large persistent

373 horizontal fracture (F2).

374 Horizontal fracture, F2, forms a laterally-persistent horizon, truncating F1 and separating

375 beds of lower and upper unit of LFA 1 (**Figure 4c, i**). F2 can be traced discontinuously

376   along the cliff sections typically up to 2 m above the level of the foreshore. Dip and dip

377   azimuth measurements collected on the fracture surfaces demonstrate a spread polymodal

378   distribution with shallow (<14 ˚) dips (**Figure 5**) indicating a gently undulating sub-

379   horizontal fracture plane.

380   The F3 fracture set extend upwards from the sub-horizontal fracture F2 occurring within the

381   upper unit of LFA 1 and also in LFA 2, but are cross-cut in-turn by LFA 3 and 4. This

382   demonstrates, that F3 post-date F2 but pre-date the deposition of LFA 3 and 4. They are

383   visible discontinuously along the length of the section, and are sub-vertically inclined (>78˚)

384   and have a marked straightness and parallelism (**Figure 5**). They range in length from 10 cm

385   to 4 m and strike broadly east northeast - west southwest.

386   Fractures F4 occur only within the cliff promontories where they truncate the entire vertical

387   section (including F1-F3) with their bases occurring beneath beach level. The fractures are

388   slightly curved fractures that radiate upwards, sub-parallel to the margins of the

389   promontories. The fractures widen upwards (up to 2 m) and towards the promontory

390   margins.

391   *Fracture Interpretation*

392   Fractures F1-F3 are interpreted as extensional fractures (mode 1 fractures) due to the lack of

393   evidence for slip or displacement along the joints. Collectively they are interpreted to form

394   broadly perpendicular sets of sub-vertical (F1 and F3) and horizontal (F2) joints formed by

395   glacier unloading, consolidation and drying of the diamicton. Sub-horizontal joints (F2) are

396   unloading joints (also called release joints) formed as the applied vertical load (ice

397   overburden) was removed. The removal of the overburden caused the vertical compressive

398   stress to be released resulting in fracturing being initiated probably along a pre-existing

399   plane of weakness. The continuous nature of F2 implies that this pre-existing plane of

400   weakness was laterally extensive, for example a shear plane, which bounded two beds of

401   LFA 1.

402   The origin of vertically-aligned fractures (F1 and F3) is also interpreted to be an artefact of

403   unloading but also subsequent drainage, drying (Boulton and Paul, 1976) and shrinkage of

404   the sediment (Mertens *et al*., 2003). Within this scenario, removal of the ice overburden led

405   to a reduction in the differential stress and a switch from dominant vertical to horizontal

406   compression (Maltman, 1994). Subsequent reduction in the horizontal compression and a

407   switch to tensile stresses would have promoted shrinkage which in-turn would require a

408   moderate differential stress to be maintained to prevent shearing (Mertens *et al*., 2003;

409   Dehandschuttter *et al*., 2005).

410   F4 fractures are focussed around the coastal spurs or promontories and cross-cut all other

411   parts of the sequence demonstrating that these are the last features to have formed. Their

412   geometry, sub-parallel alignment to the margins of the promontories and the upwards-

413   widening of the fractures, suggests that they formed by the lateral release of an applied load

414   (i.e. the removal of cliff material by coastal erosion; Cossart *et al*., 2008; Genter *et al*.,

415   2004).

416

417   **5. RESULTS: CLAST PROVENANCE**

418   *5.1 Clast lithological analysis*

419   Clast lithological data (**Table 2)** shows average percentages for each LFA. Eight samples

420   were analysed in total, four from LFA 1, three from LFA 2, and one sample from LFA 3.

421   **Figure 7** shows the results of clast lithological analysis for each sample. Representative

422   photographs are shown in **Figure 8**. The dominant lithologies within LFA 1 are

423   Carboniferous Sandstone (13.6 %), Jurassic Mudstone (11. 7 %), Cretaceous chalk (10.4 %),

424 Carboniferous Limestone (9.5 %), Magnesian Limestone (6.6 %), and Jurassic Sandstone (6.

425 2 %), (**Figure 7**). Other clast lithologies within LFA 1 include Mercia Mudstone (3.02 %),

426 Old Red Sandstone (2.9 %), Sherwood Sandstone (2.7 %), and coal (2.1 %). There are

427 relatively low amounts of Whin Sill dolerite (1.9 %), greywacke (1.2 %), diorite (0.8 %),

428 Jurassic limestone (0.6 %), andesite (0.6 %), and rhyolite (0.5 %). Notably, there is a lack of

429 distinctive Lake District granites and erratics.

430 LFA 2 contains higher percentages of Carboniferous sandstone (18.4 %), undistinguished

431 arkosic sandstone (4.6 %), Whin Sill Dolerite (4.3 %) and Sherwood Sandstone (3.1 %),

432 than LFA 1, but lower amounts of Carboniferous limestone (7.4 %), Jurassic mudstone (7.0

433 %) and Cretaceous chalk (6.6 %). There are slightly higher percentages of igneous

434 lithologies present within LFA 2, such as micro-granite (1.1 %), rhyolite (1.1 %), andesite

435 (1.0 %), basaltic porphyry (1.0 %), rhyolitic porphyry (0.6 %), andesitic porphyry (0.8 %)

436 and gabbro (0.3 %).

437 LFA 3 is dominated by a high proportion of Carboniferous sandstone (26.5 %) (**Figure 7**).

438 Other lithologies present in significant amounts are Jurassic mudstone (6.5 %), Old Red

439 Sandstone (6.2 %), yellow sandstone (5.4 %), red siltstone (5.0 %), and Jurassic sandstone

440 (3.1 %), plus an elevated amount of Whin Sill dolerite (9.6 %), much higher than is present

441 in either LFA 1 (1.9 %) or LFA 2 (4.3 %).

442   *5.2 Clast durability*

443 The two till units at Tunstall contain striated, faceted, far-travelled, non-durable erratics as

444 well as a matrix-supported sediment, indicating that a diverse suite of bedrock (including

445 softer lithologies of chalk and coal) have been eroded subglacially, cannibalised and

446 incorporated into the sediment. This suggests that the genesis of both tills was largely the

447 result of comminution and soft-sediment mixing (Roberts *et al*., 2013). The mixed

448   lithological assemblages within LFA 1 and 2 suggest subglacial cannibalism from a number

449   of different regions. CLA confirms that both tills have not been deposited close to their

450   sediment provenance areas since their lithological composition is heterogenous, indicating

451   an increasing number of sources rocks over which the glacier has travelled (cf. Boulton,

452   1996a, b). It is unlikely that the abundance of soft, non-durable, sedimentary lithologies

453   (**Figure 9**) including Jurassic, Permian and Carboniferous limestone, Jurassic mudstone,

454   coal and chalk would have survived multiple episodes of re-working, particularly within a

455   highly abrasive, subglacial environment (cf. Lee *et al*., 2002).

456   LFA 3 contains a diverse suite of erratics similar to those in LFA 1 and LFA 2 but there is a

457   noticeable paucity of non-durable lithologies such as Cretaceous chalk, Permian Magnesian

458   Limestone, and Jurassic Mudstone (**Figure 9**). The major lithological difference between

459   LFA 3 and LFA 1 and 2 is the marked increase in Whin Sill dolerite (~10 %) in LFA 3,

460   compared with <5 % in both LFA 1 and LFA 2. Almost the entire lithological content of

461   LFA 3 consists of far-travelled, durable lithologies (**Figure 9**). The presence of durable

462   lithologies support the interpretation of a high-energy environment as softer, non-durable

463   sedimentary lithologies are likely to have been destroyed by abrasion and attrition. The coal

464   fragments observed in LF 3b are an anomaly since coal is a low-durability material.

465   However, the relative buoyancy of coal aids its preservation during high-energy transport

466   whilst its deposition implies a rapid reduction (still-water) in energy regime (cf. Lee *et al*.,

467   2015).

468   *5.3 Principal Component Analysis (PCA)*

469   PCA was undertaken on the clast lithologies in an attempt to identify lithological similarities

470   between samples and determine the significant lithological variables and their

471   interrelationship. In total eight different principal components (PC 1 – 8) collectively

472   account for the lithological variability within the dataset. Three principal components (PC 1

473 – 3) account for 99.2 % of the total variability within the dataset. PC 1 explains 94.3 % of

474 the sample variation, whilst PC 2 accounts for 3.6 %, and 1.3 % is accounted for by PC 3.

475 **Figure 10a, b, c** shows the differences between lithofacies samples in relation to the

476 principal component scores (PC 1 – 3). Samples with similar clast compositions are

477 expected to cluster close together. PC 1 does not discriminate between the till samples (LFA

478 1 and 2) and the clast lithofacies (LF 3c) (**Figure 10a**). The samples do not cluster into

479 distinct groups, and the variation between samples in each LFA is large, indicating a broad

480 clast lithological spread throughout the samples. LFA 3 plots individually (**Figure 10a, c**),

481 due to the fact it has fewer non-durable lithologies (**Figure 9**). All other samples show

482 stronger variations along the axis of PC 1.

483 Based upon PC 1 there appear to be no major discernible differences in till lithology evident

484 between LFA 1 and LFA 2. However, there are subtle variations (inverse relationships)

485 between the other principal components (PC 2 and PC 3; **Figure 10b** and **c).** The principal

486 component scores suggest the correlation of samples with the established regional

487 lithostratigraphy (Skipsea and Withernsea Till) cannot be defined by bulk lithology (e.g. PC

488 1) mirroring results from other geochemical data analyses (Boston *et al*., 2010). The

489 inability of the method to discriminate between the two tills could be a consequence of the

490 small sample number taken from each of the lithofacies as this can create an artificially high

491 skew. Additionally, the stratigraphic position of LFA 2 cropping-out above LFA 1 is also

492 likely to affect its lithological composition, since the bedrock would have already been

493 mantled with till, and a re-advance would at least locally cannibalise the underlying till. The

494 lithology of LFA 2 differs slightly, as shown by the more durable clast content (**Figure 9**).

495 PC 2 however, is able to discriminate between LFA 3 and the other till samples.

496 The principal component coefficients also identify key relationships between the main

497 source provinces for the clast lithologies (**Figure 10d, e, f**). PC 1 highlights the abundance

498   of Carboniferous and Jurassic material relative to other clast lithologies, accounting for 94.3

499   % of the lithological variability within the samples. PC 2 (3.6 %) shows an inverse

500   relationship between Carboniferous, Old Red Sandstone (positive), and Jurassic, Permian,

501   and Cretaceous lithologies (strongly negative). PC 3 (1.3 %) demonstrates an inverse

502   relationship between Carboniferous and Triassic lithologies (strongly positive) and Whin

503   Sill dolerite and Old Red Sandstone (strongly negative). Collectively, the principal

504   component coefficients demonstrate complex shifts in clast lithological variability

505   throughout the Tunstall sequence. Different processes relate to the suite of clasts present in

506   each LFA, particularly between the tills (LFA 1 and 2) and glaciofluvially transported

507   material (LFA 3). Whilst clast preservation during transportation is likely to play a

508   significant role, it is likely that the relationships observed reflect considerable temporal and

509   spatial variability (including intra-till) in the entrainment of materials from the subglacial

510   bed along the ice flow path. This may reflect a temporal and spatial partitioning within the

511   subglacial bed, both in terms of areas of bedrock cover and zones of subglacial erosion, with

512   areas of the subglacial bed either buried by younger superficial deposits or strain rates being

513   too low to drive erosion. A zonal approach to glacial erosion likely relates to the suite of

514   clasts found within the tills, whereas the lack of local lithologies within LFA 3 is likely a

515   result of high energy transport.

516   *5.4 Till provenance*

517   In both till units, LFA 1 and LFA 2, Carboniferous and Jurassic components constitute >50

518   % of the lithological composition of the samples (**Figure 7**). There has been an abundant

519   incorporation of Carboniferous sandstone, limestone and coal, which are characteristic of

520   the bedrock strata from North Yorkshire, County Durham and Northumberland (Taylor and

521   Eastwood, 1971; Jones *et al*., 1995). Far-travelled sedimentary lithologies include the

522   Magnesian limestone (Cadeby Formation), which crops out extensively across north

523   Yorkshire, southern County Durham and offshore (Smith, 1995). Jurassic components are

524   traced back to outcrops in the regional area of the Cleveland basin and Redcar mudstone

525   formations in the Tees Bay (Macklin, 1998) and around Middlesbrough (Kent, 1980). Albeit

526   in low abundance in the tills, oolitic limestone is also typical of the Jurassic strata in the

527   northern part of the Cleveland basin. The Permo-Triassic Sherwood Sandstone Group

528   outcrops from the Tees Estuary to the Vale of York and the Midland Valley of Scotland

529   (Cameron and Stephenson, 1985).

530   Rare, far-travelled erratics in LFA 1 and LFA 2 include Lower Palaeozoic greywacke

531   (**Figure 8a**), which is likely to have been derived from the Southern Uplands (Greig and

532   Pringle, 1971). Devonian Old Red Sandstone clasts (**Figure 8c**) are likely to have a

533   provenance from the Midland Valley of Scotland (Trewin, 2002). Crystalline, metamorphic

534   lithologies such as schist, gneiss, diorite and k-feldspar rich granites and granodiorites

535   characteristic of the Scottish Grampian Highlands are present (**Figure 8g**, **j, k**), but in

536   extremely low abundance. This might suggest that these clasts have been re-worked from

537   the widespread Old Red Sandstone conglomerates that contain Dalradian material in the

538   Midland Valley (Cameron and Stephenson, 1985) or that their proportions have been diluted

539   by the incorporation of more local materials. K-feldspar granite clasts could also be derived

540   from the Cheviot Hills. Both tills contain purple to reddish-brown rhyolites, greenish-brown

541   andesites and porphyries (**Figure 8d**, **h**), which are characteristic of the Devonian Cheviot

542   Volcanic Formation that straddles the border between Northumberland and Scotland

543   (Toghill, 2011; Robson 1976). Rhyolite and andesite can also be attributed to the Lake

544   District, but the reddish-pink nature of the majority of rhyolites from Tunstall (e.g. **Figure**

545   **8h**) indicate a stronger presence of feldspar, characteristic of outcrops in the Cheviot Hills

546   (Robson, 1976). The Cheviot Hills is, therefore, established as the principal source region

547 for many of the igneous lithologies due to the large extent of felsic intrusive material in this

548 area.

549 The overall lithological composition of both tills (LFA 1 and LFA 2) suggest that they were

550 deposited by ice that flowed southwards down the present east coast of England. Source

551 regions for the ice, indicated by the clast lithological composition, include the Midland

552 Valley of Scotland, Southern Uplands and East Grampian Highlands, before ice entrained

553 erratics from the Cheviots, Northumberland and Durham (**Figure 11**) moving southwards to

554 the Holderness area.

555

556 **6. DISCUSSION**

557 *6.1 Implications for the Devensian Stratigraphy of eastern England*

558 LFA 1 and 2 are both massive, matrix-supported diamictons. At the macroscale, both units

559 appear to possess a similar texture, particle size distribution and clast content. A chi-square

560 test on the particle size distribution (**Table 1**) demonstrate that both tills cannot be

561 differentiated on the basis of particle size ($\chi^2{}_{calc}$ (0.002) < $\chi^2{}_{crit}$ (0.35)), meaning that they

562 could originate from the same source material. Other similarities between LFA 1 and 2

563 include laminations of gravel that are observed sporadically within both units and stringers

564 that also occur at the base of both LFA 1 and 2. However, there are also subtle meso-scale

565 (cm to m) variations between LFA 1 and 2 and distinguishing characteristics are matrix

566 colour and fracture density. Along the length of the section there is only one short exposure

567 where the lower two LFAs can be observed in superposition (**Figure 3b;** section log 5;

568 **Figure 4i**). At this boundary, the contact between the units is sharp and highly fissile. There

569 are also sand and gravel interbeds at the contact. The colour contrast at this boundary

570 between LFA 1 and 2 is sharp. LFA 1 is darker in colour, particularly at the base, due to

571   being constantly saturated with water from the sea at high tide. Fissile structures are more

572   abundant within LFA 1 than LFA 2, particularly at the contact where the upper contact with

573   LFA 2 is sharp with a concave base. LFA 1 is slightly more stone-rich and more heavily

574   fractured at the base than LFA 2 (**Figure 4i**).

575   Previous interpretations of the stratigraphic sequences along the Holderness coast have

576   suggested that two Late Devensian tills are present - the Skipsea and Withernsea tills (Catt

577   and Penny, 1966; Madgett and Catt, 1978; Bell and Forster, 1991; Bowen, 1999; Bell, 2002;

578   Catt, 2007). These classifications are founded largely on the basis of changes in matrix

579   colour and clast lithological assemblage (Catt and Penny, 1966; Madgett and Catt, 1978;

580   Bowen, 1999; Catt, 2007). In this study, LFA 1 is interpreted as a subglacial traction till

581   equivalent to the Skipsea Till on the basis of its dark brown colour, greater chalk content,

582   and northern clast erratic assemblage. This interpretation is regionally supported by other

583   investigations of tills which correlate stratigraphically to the Skipsea Till, such as the

584   Horden Till Formation at Whitburn Bay (Davies *et al*., 2009), other areas of east Yorkshire

585   (Catt, 2007; Boston *et al*., 2010; Evans and Thomson, 2010), Northumbria (Eyles *et al*.,

586   1982), and offshore (Carr *et al*., 2006; Davies *et al*., 2011). Based on its stratigraphic

587   position (overlying the Skipsea Till), LFA 2 should therefore be assigned to the Withernsea

588   Till. Sedimentologically, LFA 2 is similar to previous descriptions of the Withernsea Till; it

589   is a dark reddish brown sandy diamicton. However, the lithological data presented in this

590   study does not support the concept of LFA 2 being an entirely different till, as its bulk

591   lithology is indistinctive from the Skipsea Till.

592   The till sequences that crop-out along the east coast of England have consistently been

593   referred to as the product of either Scottish or east coast ice from the North Sea ice lobe

594   (NSL), or Stainmore ice. Clast lithological data from this study concludes that the tills

595   possess similar lithological characteristics and provenance. Evidence of Lake District input

596   (cf. Bisat, 1939; Radge, 1939; Catt and Penny, 1966; Catt and Digby, 1988; Bell and

597   Forster, 1991) was not replicated in this study and the lithological analysis at Tunstall

598   reveals no indicator erratics from the western part of England, now widely discredited

599   nevertheless (Davies *et al.*, 2019). This confirms that the tills are not associated with the

600   same ice lobe as the Vale of York glacier that formed the York and Escrick moraines

601   (Phillips, 1827; Howarth, 1903; Melmore, 1935, p. 31) as previously thought (Ford *et al.*,

602   2008).

603   The visual difference between the two tills at Tunstall can potentially be explained by the

604   local incorporation of rafts of the Sherwood Sandstone and /or Mercia Mudstone group (or

605   rafts of till units rich in these materials). Intermixing of the two tills (e.g. **Figure 4d, e**)

606   demonstrates that colour changes likely reflect subtle differences in till composition and

607   sediment source rather than weathering. Similar red diamictons and sands interbedded with

608   grey diamictons also occur within Devensian tills at Warren House Gill in Country Durham

609   (Davies *et al.*, 2012), indicating that this is a regional phenomenon. Whilst locally, this may

610   enable the apparent sub-division of till units into Skipsea and Withernsea Till facies, at other

611   sites to the north in Holderness (e.g. between Mappleton and Skipsea), facies of 'Withernsea

612   Till' occur within the 'Skipsea Till' (Jonathan Lee, unpublished data). Principal

613   Components Analysis also reveals subtle clast lithological variations within the till units

614   demonstrating greater intra- rather than inter- till variability. Therefore, on the basis of clast

615   lithological composition alone, it is difficult to discriminate between the two subglacial tills

616   identified at Tunstall. In simple terms, there is not a consistent superpositional relationship

617   between 'Skipsea Till' and 'Withernsea Till' facies in the Tunstall area and thus the

618   lithostratigraphic scheme becomes unviable. This lithological analysis supports the findings

619   from Boston *et al.* (2010), where geochemical analysis of LGM tills and glaciotectonites in

620   east Yorkshire and Lincolnshire failed to precisely differentiate the Skipsea and Withernsea

621 Till types. This makes the application of the traditional nomenclature over a wider regional

622 area tenuous.

623 Given that the stratigraphic succession at Tunstall cannot be assigned to the traditional

624 bipartite sequence, we propose that inter- and intra-till variability relates to changes in

625 subglacial debris provenance. Variations in debris provenance can be explained by both

626 temporal and spatial changes in the availability of source materials implying that geological

627 sources cycled through phases of active and non-entrainment. This entrainment could occur

628 by melt and refreeze at the margins of the glacier prior to advance, by active shearing of

629 overridden stony permafrost, from supraglacial sources, or by normal melt-freeze

630 entrainment processes in temperate ice (Alley *et al*., 1997) whereby the glacier actively

631 entrains basal material derived from the substrate by abrasion. To readily entrain debris into

632 the basal layers of glacial ice, debris entrainment encompasses the detachment of frozen

633 blocks of sediment from the subglacial substrate which is then folded and thrusted. The

634 general entrainment mechanisms for basal debris transportation make these units

635 rheologically distinct. It is suggested that this behaviour may relate to changes in subglacial

636 conditions and behaviour. For example, the temporary burial (or exposure) of a specific

637 source material and/or changes in the subglacial bed rheology which drive stick (erosion)

638 and slip (non- or reduced entrainment) ice flow (Iverson, 2010; Iverson and Peterson, 2011;

639 Phillips *et al*., 2018).

640 *6.2 Genetic Model: the significance of fractures F1 – F3*

641 Fractures F1-F3 are interpreted as being formed in response to unloading and shrinkage of

642 the tills in response to the removal of overlying glacier ice, followed by consolidation and

643 drying. F2 fractures are interpreted as unloading joints aligned perpendicular to the direction

644 of unloading (vertical). The geometry of the F2 fracture implies that the fracture developed

645 on a pre-existing, regionally-extensive plane of weakness such as a décollement surface.

646   The simplest interpretation is that this décollement surface originally formed due to the low-

647   angle glaciotectonic thrust emplacement of a layer of LFA 1 on top of LFA 1 (cf. Hiemstra

648   *et al*., 2007; Lee *et al*., 2013, 2017). The low-angle geometry of the décollement surface

649   implies that porewater pressures along the detachment were elevated (Phillips *et al*., 2008;

650   Lee *et al*., 2013, 2017). However, the sharpness of the fracture and absence of dewatering

651   structures (e.g. diffuse bedding, flame structures) suggests that a degree of consolidation and

652   dewatering of the lower unit of LFA 1 had occurred prior to thrusting indicating a possible

653   hiatus. Vertical fractures F1 and F3, produced during unloading and subsequent shrinkage,

654   are partitioned by sub-horizontal fracture F2. These fractures could have developed broadly

655   contemporaneously with F2 acting to partition stress, restricting the spatial development of

656   F1 and F3. Alternatively, F1 could predate F2, and F3 post-date F2. This would lend further

657   support to the interpretation that F2 is superimposed upon a relict thrust plane and that a

658   hiatus occurred during the accretion of LFA 1 resulting in partial consolidation and drying.

659   These characteristics, coupled with the emplacement of LFA 2 over LFA 1, are considered

660   to suggest a highly-dynamic temperate ice-marginal landsystem (cf. Evans and Twigg,

661   2002), characterised by multiple ice-marginal oscillations that resulted in the thrust-stacking

662   of multiple till blocks.

663   Till sequences produced by thrust-stacking typically create vertical, repetitive

664   sedimentological/lithological signatures observed frequently in exposures of glacial geology

665   elsewhere along the east coast of Britain (Boston *et al*., 2010; Evans and Thomson, 2010;

666   Lee *et al*., 2013, 2017). Although there are undoubtedly two till units (LFA 1 and LFA 2)

667   present at Tunstall, they have both been deposited by the NSL and reflect repeated ice-

668   marginal oscillations and till emplacement by thrust-stacking. We propose that the sequence

669   at Tunstall was generated by successive ice-margin oscillations, and are thereby suggestive

670   of active retreat (Boulton, 1996a, b; cf. Dove *et al*., 2018). Alternatively, as the substrate is

671 progressively buried by surficial deposits following each advance-retreat phase, the stacked

672 sequence could be a function of reduced interaction of basal ice with the local lithologies

673 (Boulton, 1996a, b; Kjær *et al*., 2006). In this case, the frequency of far-travelled

674 lithological components of the till would increase with height and produce a similar

675 lithological heterogeneity within samples, such as the results of this study.

676   *6.3 A litho-tectonic event model for Tunstall*

677 The fracture sets, lithological and sedimentological data from Tunstall enable an integrated

678 litho-tectonic model for the site to be proposed (**Table 3**). In summary, the vertical and

679 horizontal fractures provide a complementary record to the sedimentological and

680 lithological analysis suggesting multiple phases of ice advance and retreat: (i) ice advance

681 and accretion of the lower part of LFA 1; (ii) ice-marginal retreat, unloading, consolidation

682 and shrinkage (formation of F1); (iii) brief hiatus; (iv) ice-marginal re-advance, thrust

683 stacking of LFA 1 on top of LFA 1; (v) ice marginal retreat, unloading and horizontal

684 fracturing (F2) developed along a pre-existing decollement surface; (vi) ice-marginal re-

685 advance, emplacement of LFA 2; (vii) ice-marginal retreat, unloading, consolidation and

686 shrinkage – formation of F3 fractures; (viii) sub-marginal deposition of glaciofluvial

687 deposits LFA 3; (ix) non-glacial deposition of LFA 4 (x) coastal erosion and development of

688 lateral release joints (formation of F4).

689 The application of lithostratigraphic principals to the Skipsea Till significantly under-

690 represents the geological relevance of the 'unit' and specifically the number of ice-advances

691 that formed the unit. This mirrors studies utilising glaciotectonic evidence elsewhere in

692 eastern England, which records considerably much more dynamic phase of ice-marginal

693 behaviour than shown by lithostratigraphic data alone (Lee and Phillips, 2008; Phillips *et*

694 *al*., 2008; Lee *et al*., 2013; Phillips and Lee, 2013; Lee *et al*., 2017).

695 The presence of two distinctly different till units – the Skipsea and Withernsea tills, is also

696 questioned based on lithological data. Instead the till units are interpreted as thrust-induced

697 stacks of pre-existing till that accreted during cyclical oscillations of the ice margin (cf.

698 Hiemstra *et al*., 2007; Lee *et al*., 2017) and up-ice variations in subglacial entrainment of

699 bedrock lithologies. We therefore propose the term 'Skipsea till complex' to encompass the

700 multiple thrust-stacked layers of till which cannot be classified lithostratigraphically.

701

702 **7. CONCLUSIONS**

703 The stratigraphic succession at Tunstall contains four lithofacies associations (LFA 1 - 4)

704 and three primary fracture sets (F1 - F3) which collectively establish an event stratigraphy

705 for the site encompassing the Late Devensian glaciation. The succession records two

706 superimposed subglacial traction till units (LFA 1 and 2). Sub-horizontal fracture (F2) is

707 interpreted as an unloading joint superimposed upon a regionally-extensive décollement

708 surface formed during the thrust-stacking of a unit of LFA 1 on top of LFA 1. Vertical

709 fractures F1 and F3 appear to relate to shrinkage and are tentatively interpreted to indicate

710 two separate phases of unloading and shrinkage that occurred following ice-marginal retreat

711 intra-LFA 1 and following the accretion of LFA 2. LFA 3 and 4 record the transition to non-

712 glacial conditions.

713 Clast lithological data have also been used to reconstruct glacial transport pathways for the

714 tills at Tunstall during the Late Devensian glaciation. The data provide evidence in support

715 of deposition by a lobe of glacier ice (first sourced from southern and central Scotland), that

716 flowed southwards down the present east coast of England (and offshore area of the

717 southern North Sea) before reaching its final extent on the Holderness coast. The

718 provenance of both tills therefore indicate an exclusively northern British origin. However,

719   statistical analysis of the clast lithological data demonstrates that there is greater intra-till

720   lithological variability within the tills than between the till units. We suggest this

721   lithological variability reflects temporal and spatial variability in the availability and

722   entrainment of bedrock source materials along the ice flow path. Furthermore, the two

723   subglacial tills at Tunstall cannot be differentiated lithostratigraphically, nor can they be

724   directly correlated with the regional glacial lithostratigraphy along the east and northeast

725   coast of Britain. This supports similar assertions made previously by Boston *et al*. (2010)

726   based on geochemical analysis from the Holderness tills.

727   Collectively, this evidence demonstrates that caution is required when applying

728   lithostratigraphic principals to till because these can underestimate the history of ice

729   advance and dynamic ice-marginal behaviour. In the case of this study, we consider that

730   variations in till lithological properties are not clear-cut between till units. Instead, the

731   variability in till composition reflects the temporal and spatial patterns of up-ice source

732   material entrainment plus the local erosional processes driven by thrust-stacking at an

733   oscillating ice margin.

734

735   **ACKNOWLEDGEMENTS**

743   anonymous reviewer and Clare Boston for providing constructive reviews on the

744   manuscript.

745

746 **REFERENCES**

747 Andrews, J. E., Pedley, M., and Dennis, P. F. 2000. Palaeoenvironmental records in

748   Holocene Spanish tufas: a stable isotope approach in search of reliable climatic

749   archives. *Sedimentology*, *47*(5), 961-978

750 Bamber, J. L., Riva, R. E., Vermeersen, B. L., and LeBrocq, A. M. 2009. Reassessment of

751   the potential sea-level rise from a collapse of the West Antarctic Ice

752   Sheet. *Science*, *324*(5929), 901-903

753 Bateman, M. D., Buckland, P. C., Whyte, M. A., Ashurst, R. A., Boulter, C., and

754   Panagiotakopulu, E. V. A. 2011. Re-evaluation of the Last Glacial Maximum

755   typesite at Dimlington, UK. *Boreas*, *40*(4), 573-584

756 Bateman, M. D., Evans, D. J. A., Buckland, P. C., Connell, E. R., Friend, R. J., Hartmann,

757   D., Moxon, H., Fairburn, W. A., Panagiotakopulu, E., and Ashurst, R. A. 2015. Last

758   glacial dynamics of the Vale of York and North Sea lobes of the British and Irish

759   Ice Sheet. *Proceedings of the Geologists' Association*, *126*(6), 712-730

760 Bateman, M. D., Evans, D. J., Roberts, D. H., Medialdea, A., Ely, J., and Clark, C. D. 2017.

761   The timing and consequences of the blockage of the Humber Gap by the last

762   British− Irish Ice Sheet. *Boreas 47,* 41-61

763 Bell, F. G., and Forster, A. 1991. The geotechnical characteristics of the till deposits of

764   Holderness. *Geological Society, London, Engineering Geology Special*

765   *Publications*, *7*(1), 111-118

766 Benn, D. I. 1994. Fabric shape and the interpretation of sedimentary fabric data. *Journal of*

767   *Sedimentary Research*, 64(4), 910-915

768   Bennett, M. R., Waller, R. I., Glasser, N. F., Hambrey, M. J., and Huddart, D. 1999.

769   Glacigenic clast fabrics: genetic fingerprint or wishful thinking? *Journal of*

770   *Quaternary Science*, *14*(2), 125-135

771   Bird, E. ed., 2010. *Encyclopedia of the world's coastal landforms*. Springer Science and

772   Business Media

773   Bisat, W. S. 1939. Older and newer drift in East Yorkshire. In *Proceedings of the Yorkshire*

774   *Geological and Polytechnic Society, Geological Society of London, 24(3),* 137-151

775   Boston, C. M., Evans, D. J. A., and Ó Cofaigh, C. 2010. Styles of till deposition at the

776   margin of the Last Glacial Maximum North Sea lobe of the British–Irish Ice Sheet:

777   an assessment based on geochemical properties of glacigenic deposits in eastern

778   England. *Quaternary Science Reviews*, *29*(23), 3184-3211

779   Boulton, G. S. 1996a. The origin of till sequences by subglacial sediment deformation

780   beneath mid-latitude ice sheets. *Annals of Glaciology*, *22*(1), 75-84

781   Boulton, G. S. 1996b. Theory of glacial erosion, transport and deposition as a consequence

782   of subglacial sediment deformation. *Journal of Glaciology*, *42*(140), 43-62

783   Boulton, G.S., and Paul, M.A. 1976. The influence of genetic process on some

784   geotechnical properties of glacial tills. *Quarterly Journal of Engineering Geology*,

785   9, 159-194

786   Boulton, G. S., and Hindmarsh, R. C. A. 1987. Sediment deformation beneath glaciers:

787   rheology and geological consequences. *Journal of Geophysical Research: Solid*

788   *Earth*, *92*, 9059-9082

789   Bridgland, D. R. 1986. *Clast lithological analysis* (No. 3). Quaternary Research

790   Association

791   Busfield, M. E., Lee, J. R., Riding, J. B., Zalasiewicz, J., and Lee, S. V. 2015. Pleistocene

792   till provenance in east Yorkshire: reconstructing ice flow of the British North Sea

793   Lobe. *Proceedings of the Geologists' Association*, *126*(1), 86-99

794   Cameron, I. B., and Stephenson, D. 1985. *British regional geology: the Midland Valley of*

795   *Scotland* (No. 5). Hmso Books

796   Carr, S. J., Holmes, R. V. D., Van der Meer, J. J. M., and Rose, J. 2006. The Last Glacial

797   Maximum in the North Sea Basin: micromorphological evidence of extensive

798   glaciation. *Journal of Quaternary Science*, *21*(2), 131-153

799   Castedo, R., de la Vega-Panizo, R., Fernández-Hernández, M. and Paredes, C. 2015.

800   Measurement of historical cliff-top changes and estimation of future trends using

801   GIS data between Bridlington and Hornsea–Holderness Coast (UK).

802   *Geomorphology*, *230*, pp.146-160

803   Catt, J. A. 2007. The Pleistocene glaciations of eastern Yorkshire: a review. *Proceedings of*

804   *the Yorkshire Geological Society*, *56*(3), 177-207

805   Catt, J. A., and Digby, P. G. N. 1988. Boreholes in the Wolstonian Basement Till at

806   Easington, Holderness, July 1985. In *Proceedings of the Yorkshire Geological and*

807   *Polytechnic Society*, Geological Society of London, 47(1), 21-27

808   Catt, J. A., and Penny, L. F. 1966. The Pleistocene deposits of Holderness, East

809   Yorkshire. *Proceedings of the Yorkshire Geological Society*, *35*(3), 375-420

810   Cheshire, D. A. 1986. *The lithology and stratigraphy of the Anglian deposits of the Lea*

811   *basin* (Doctoral dissertation, Hatfield Polytechnic).

812   Clark, C. D., Hughes, A. L., Greenwood, S. L., Jordan, C., and Sejrup, H. P. 2012. Pattern

813   and timing of retreat of the last British-Irish Ice Sheet. *Quaternary Science*

814   *Reviews*, *44*, 112-146

815   Clark, C. D., Ely, J. C., Greenwood, S. L., Hughes, A. L. C., Meehan, R., Barr, I. D.,

816   Bateman, M. D., Bradwell, T., Doole, J., Evans, D. J. A., Jordan, C. J., Monteys, X.,

817   Pellicer, X. M., Sheehy, M., 2018. BRITICE Glacial Map, version 2: a map and GIS

818   database of glacial landforms of the last British–Irish Ice Sheet. *Boreas, 47 (1)*, 11-

819   18

820   Collinson, J. D. 1996. Alluvial Sediments. In, Reading, H. G. (ed). Sedimentary

821   environments: processes, facies and stratigraphy.

822   Cossart, E., Braucher, R., Fort, M., Bourlès, D.L. and Carcaillet, J. 2008. Slope instability

823   in relation to glacial debuttressing in alpine areas (Upper Durance catchment,

824   southeastern France): Evidence from field data and 10Be cosmic ray exposure ages.

825   *Geomorphology*, *95*(1-2), 3-26

826   Cotterill, C. J., Phillips, E., James, L., Forsberg, C. F., Tjelta, T. I., Carter, G., and Dove, D.

827   2017. The evolution of the Dogger Bank, North Sea: A complex history of

828   terrestrial, glacial and marine environmental change. *Quaternary Science*

829   *Reviews*, *171*, 136-153

830   Davies, B. J., Roberts, D. H., Ó Cofaigh, C., Bridgland, D. R., Riding, J. B., Phillips, E. R.,

831   and Teasdale, D. A. 2009. Interlobate ice-sheet dynamics during the Last Glacial

832   Maximum at Whitburn Bay, County Durham, England. *Boreas*, *38*(3), 555-578

833   Davies, B. J., Roberts, D. H., Bridgland, D. R., Ó Cofaigh, C., and Riding, J. B. 2011.

834   Provenance and depositional environments of Quaternary sediments from the

835   western North Sea Basin. *Journal of Quaternary Science*, *26*(1), 59-75

836   Davies, B. J, Roberts, D. H, Bridgland, D. R, Ó Cofaigh, C, Riding, J. B, Demarchi, B,

837   Penkman, K. E. H., and Pawley, S. M. 2012. Timing and depositional environments of a

838   Middle Pleistocene glaciation of northeast England: New evidence from Warren House Gill,

839   County Durham. *Quaternary Science Reviews, 44*, 180-212

840 Davies, B, Yorke, L, Bridgland, D and Roberts, D., (eds), 2013, *Quaternary of*

841   *Northumberland, Durham and Yorkshire*. Quaternary Research Association,

842   London, pp 208

843 Davies, B.J., Livingstone, S.J., Roberts, D.H., Evans, D.J.A., Gheorghiu, D.M. and Cofaigh,

844   C.Ó. 2019. Dynamic ice stream retreat in the central sector of the last British-Irish

845   Ice Sheet. *Quaternary Science Reviews*, *225*;

846 Davies, B.J., Livingstone, S.J., Roberts, D.H., Evans, D.J.A., Gheorghiu, D.M. and Cofaigh,

847   C.Ó., 2019. Dynamic ice stream retreat in the central sector of the last British-Irish

848   Ice Sheet. *Quaternary Science Reviews*, *225*

849 Davis, J. C. 1986: Statistics and Data Analysis in Geology. 656 pp. John Wiley & Sons

850 DeConto, R.M. and Pollard, D., 2016. Contribution of Antarctica to past and future sea-

851   level rise. *Nature*, *531*(7596), 591

852 Dehandschutter, B., Vandycke, S., Sintubin, M., Vandenberghe, N., and Wouters, L. 2005.

853   Brittle fractures and ductile shear bands in argillaceous sediments: inferences from

854   Oligocene Boom Clay (Belgium). *Journal of Structural Geology*, *27*, 1095-1112.

855 Dove, D., Evans, D. J., Lee, J. R., Roberts, D. H., Tappin, D. R., Mellett, C. L., Long, D.,

856   and Callard, S. L. 2017. Phased occupation and retreat of the last British–Irish Ice

857   Sheet in the southern North Sea; geomorphic and seismostratigraphic evidence of a

858   dynamic ice lobe. *Quaternary Science Reviews, 163*, 114-134

859 Dowdeswell, J. A., Ottesen, D., and Rise, L. 2006. Flow switching and large-scale

860   deposition by ice streams draining former ice sheets. *Geology*, *34*(4), 313-316

861   Edwards, C. A. 1981. 'The tills of Filey Bay', in Neale J. and Flenley, J. (Eds), The

862   Quaternary in Britain, Pergamon Press, Oxford.

863   Edwards, C. A. 1987. 'The Quaternary deposits in Filey Bay', in Ellis, S. (Ed.), *East*

864   *Yorkshire Filed Guide.* Quaternary Research Association, 15-21

865   Ely, J. C., Clark, C. D., Hindmarsh, R. C., Hughes, A. L., Greenwood, S. L., Bradley, S. L.,

866   Gasson, E., Gregoire, L., Gandy, N., Stokes, C. R, and Small, D. 2019. Recent

867   progress on combining geomorphological and geochronological data with ice sheet

868   modelling, demonstrated using the last British–Irish Ice Sheet. *Journal of*

869   *Quaternary Science* 1-15

870   Emery, A. R., Hodgson, D. M., Barlow, N. L., Carrivick, J. L., Cotterill, C. J., Mellett, C.

871   L., and Booth, A. D. 2019. Topographic and hydrodynamic controls on barrier

872   retreat and preservation: An example from Dogger Bank, North Sea. *Marine*

873   *Geology*, 105981

874   Evans, D. J. A. and Benn, D. I. 2004: A Practical Guide to the Study of Glacial Sediments.

875   206 pp. Arnold, London.

876   Evans, D. J. A., Bateman, M. D., Roberts, D. H., Medialdea, A., Hayes, L., Duller, G. A.,

877   and Clark, C. D. 2016. Glacial Lake Pickering: stratigraphy and chronology of a

878   proglacial lake dammed by the North Sea Lobe of the British–Irish Ice Sheet.

879   *Journal of Quaternary Science, 32(2),* 295-310

880   Evans, D. J. A., Lemmen, D. S. and Rea, B. R. 1999. Glacial landsystems of the southwest

881   Laurentide Ice Sheet: modern Icelandic analogues. *Journal of Quaternary Science,*

882   *14*, 673–691

883   Evans, D. J. A., Owen, L. A. and Roberts, D. H. 1995. Stratigraphy and sedimentology of

884   Devensian (Dimlington Stadial) glacial deposits, East Yorkshire, England. *Journal*

885   *of Quaternary Science, 10*, 241–265

886   Evans, D. J. A., Phillips, E. R., Hiemstra, J. F., and Auton, C. A. 2006. Subglacial till:

887   formation, sedimentary characteristics and classification. *Earth-Science*

888   *Reviews*, *78*(1), 115-176

889   Evans, D. J. A., and Thomson, S. A. 2010. Glacial sediments and landforms of Holderness,

890   eastern England: a glacial depositional model for the North Sea Lobe of the British–

891   Irish Ice Sheet. *Earth-Science Reviews*, *101*(3), 147-189

892   Evans, D.J.A., Twigg, D.R., 2002. The active temperate glacial landsystem: a model based

893   on Breiðamerkurjökull and Fjallsjökull, Iceland. *Quaternary Science Reviews*, 21,

894   2143-2177.

895   Evans, D. J. A,, Bateman, M. D., Roberts, D. H., Medialdea, A., Hayes, L., Duller, G. A.,

896   Fabel, D., and Clark, C. D. 2017. Glacial Lake Pickering: stratigraphy and

897   chronology of a proglacial lake dammed by the North Sea Lobe of the British–Irish

898   Ice Sheet. *Journal of Quaternary Science*, *32*(2), 295-310

899   Evans, D. J. A., Clark, C. D., and Mitchell, W. A. 2005. The last British Ice Sheet: A review

900   of the evidence utilised in the compilation of the Glacial Map of Britain. *Earth-*

901   *Science Reviews*, *70*(3), 253-312

902   Evans, D. J. A., Dinnage, M., and Roberts, D. H. 2018. Glacial geomorphology of

903   Teesdale, northern Pennines, England: Implications for upland styles of ice stream

904   operation and deglaciation in the British-Irish Ice Sheet. *Proceedings of the*

905   *Geologists' Association*, *129*(6), 697-735

906   Evans, D.J.A., Roberts, D.H., Bateman, M.D., Ely, J., Medialdea, A., Burke, M.J.,

907   Chiverrell, R.C., Clark, C.D., Fabel, D., 2019. A chronology for North Sea Lobe

908   advance and recession on the Lincolnshire and Norfolk coasts during MIS 2 and 6.

909   *Proceedings of the Geologists' Association*, 130, 523-540.

910   Evans, D.J.A., Thomson, S.A., Clark, C.D., 2001. Introduction to the Late Quaternary of

911   East Yorkshire and North Lincolnshire, in: Bateman, M.D., Buckland, P.C.,

912   Frederick, C.D., Whitehouse, N.J. (Eds.), The Quaternary of East Yorkshire and

913   North Lincolnshire. Field Guide. Quaternary Research Association, London, pp. 1-

914   12

915   Everest, J., Bradwell, T., and Golledge, N. 2005. Subglacial landforms of the tweed palaeo-

916   ice stream. *The Scottish Geographical Magazine*, *121*(2), 163-173

917   Eyles, N., Sladen, J. A., and Gilro, S. 1982. A depositional model for stratigraphic

918   complexes and facies superimposition in lodgement tills. *Boreas*, *11*(4), 317-333

919   Eyles, N., and McCabe, A. M. 1989. The Late Devensian (< 22,000 BP) Irish Sea Basin: the

920   sedimentary record of a collapsed ice sheet margin. *Quaternary Science*

921   *Reviews*, *8*(4), 307-351

922   Eyles, N., McCabe, A. M., and Bowen, D. Q. 1994. The stratigraphic and sedimentological

923   significance of Late Devensian ice sheet surging in Holderness, Yorkshire,

924   UK. *Quaternary Science Reviews*, *13*(8), 727-759

925   Fairburn, W. A., and Bateman, M. D. 2016. A new multi-stage recession model for

926   Proglacial Lake Humber during the retreat of the last British–Irish Ice

927   Sheet. *Boreas*, *45*(1), 133-151

928   Ford, J. R., Cooper, A., Price, S. J., Gibson, A., Pharaoh, T. C., and Kessler, H., 2008.

929   Geology of the Selby district: a brief explanation of the geological map Sheet 71

930   Selby. British Geological Survey, Keyworth Nottingham, HMSO

931   Gale, S., and Hoare, P. G. 2012. *Quaternary sediments: petrographic methods for the study*

932   *of unlithified rocks*. Blackburn Press

933   Gandy, N., Gregoire, L.J., Ely, J., Clark, C., Hodgson, D.M., Lee, V., Bradwell, T. and

934   Ivanovic, R.F. 2018. Marine ice sheet instability and ice shelf buttressing of the

935   Minch Ice Stream, northwest Scotland. *The Cryosphere*, *12*; 3635-3651

936   Gandy, N., Gregoire, L.J., Ely, J.C., Cornford, S.L., Clark, C.D. and Hodgson, D.M. 2019.

937   Exploring the ingredients required to successfully model the placement, generation,

938   and evolution of ice streams in the British-Irish Ice Sheet. *Quaternary Science*

939   *Reviews*, *223*;

940   Garnett, E. R., Gilmour, M. A., Rowe, P. J., Andrews, J. E., and Preece, R. C. 2004. 230

941   Th/234 U dating of Holocene tufas: possibilities and problems. *Quaternary Science*

942   *Reviews*, *23*(7), 947-958

943   Gaunt, G. 1975. The Devensian maximum ice limit in the Vale of York. Proceedings of the

944   Yorkshire Geological and Polytechnic Society, Geological Society of London

945   Genter, A., Duperret, A., Martinez, A., Mortimore, R.N. and Vila, J.L. 2004. Multiscale

946   fracture analysis along the French chalk coastline for investigating erosion by cliff

947   collapse. *Geological Society, London, Engineering Geology Special Publications*,

948   *20*(1), 57-74

949   Gibbard, P. L. 1985. *The Pleistocene History of the Middle Thames Valley*. Cambridge

950   University Press

951   Gibbard, P. L. 1986. Comparison of the clast lithological composition of gravels in the

952   Middle Thames using canonical variates analysis and principal components

953   analysis. *Clast Lithological Analysis. Technical Guide*, (3)

954   Greig, D. C., and Pringle, J. 1971. *British regional geology: the south of Scotland*. HMSO

955   Hambrey, M. J., and Glasser, N. F. 2012. Discriminating glacier thermal and dynamic

956   regimes in the sedimentary record. *Sedimentary Geology*, *251*, 1-33

957   Hart, J. K. 1997. The relationship between drumlins and other forms of subglacial

958   glaciotectonic deformation. *Quaternary Science Reviews*, *16*(1), 93-107

959   Hicock, S. R., and Fuller, E. A. 1995. Lobal interactions, rheologic superposition, and

960   implications for a Pleistocene ice stream on the continental shelf of British

961   Columbia. *Geomorphology*, *14*(2), 167-184

962   Hiemstra, J. F., Evans, D. J., and Ó Cofaigh, C. 2007. The role of glacitectonic rafting and

963   comminution in the production of subglacial tills: examples from southwest Ireland

964   and Antarctica. *Boreas*, *36*(4), 386-399

965   Hubbard, A., Bradwell, T., Golledge, N., Hall, A., Patton, H., Sugden, D., Cooper, R., and

966   Stoker, M. 2009. Dynamic cycles, ice streams and their impact on the extent,

967   chronology and deglaciation of the British–Irish ice sheet. *Quaternary Science*

968   *Reviews*, *28*(7), 758-776

969   Hubbard, B., and Glasser, N. F. 2005. *Field techniques in glaciology and glacial*

970   *geomorphology*. John Wiley & Sons

971   Hughes, A. L., Gyllencreutz, R., Lohne, Ø. S., Mangerud, J., and Svendsen, J. I. 2016. The

972   last Eurasian ice sheets–a chronological database and time-slice reconstruction,

973   DATED-1. *Boreas 45(1),* 1-45

974   Iverson, N.R. 2010. Shear resistance and continuity of subglacial till: hydrology rules.

975   *Journal of Glaciology*, *56*(200), 1104-1114

976   Iverson, N.R. and Petersen, B.B. 2011. A new laboratory device for study of subglacial

977   processes: first results on ice–bed separation during sliding. *Journal of Glaciology*,

978   *57*(206), 1135-1146

979   Jones, J.M., Magraw, D., O'Mara, P.T., 1995. "Carboniferous and Westphalian coal

980   measures". In Johnson, G.A.L., 1995 (ed.), "Robson's Geology of northeast

981   England". *Transactions of the Natural History Society of Northumbria,* Volume 56,

982   Part 5, p. 267-282.

983   Kent, P., 1980. British regional Geology: Eastern England from the Tees to the Wash.

984   *Institute of Geological Sciences.* Natural Environment Research Council. HMSO,

985   London. Pp. 155

986   Kerney, M. P., Preece, R. C., and Turner, C. 1980. Molluscan and plant biostratigraphy of

987   some Late Devensian and Flandrian deposits in Kent. *Philosophical Transactions of*

988   *the Royal Society of London. Series B, Biological Sciences*, 1-43

989   Kjær, K. H., Larsen, E., van der Meer, J., Ingólfsson, Ó., Krüger, J., Benediktsson, Í. Ö.,

990   Knudsen, C. G., and Schomacker, A. 2006. Subglacial decoupling at the

991   sediment/bedrock interface: a new mechanism for rapid flowing ice. *Quaternary*

992   *Science Reviews*, *25*(21), 2704-2712

993   Kovach, W. L. 1995: Multivariate analysis. In Maddy, D. and Brew, J. S. (eds.): *Statistical*

994   *Modelling of Quaternary Science Data*, 1–38. Technical Guide 5, Quaternary

995   Research Association, Cambridge

996   Lee, J. R., Rose, J., Riding, J. B., Moorlock, B. S., and Hamblin, R. J. 2002. Testing the case

997   for a Middle Pleistocene Scandinavian glaciation in Eastern England: evidence for a

998   Scottish ice source for tills within the Corton Formation of East Anglia,

999   UK. *Boreas*, *31*(4), 345-355

1000   Lee, J. R. 2003. *Early and Middle Pleistocene lithostratigraphy and palaeo-environments in*

1001   *northern East Anglia* (Doctoral dissertation, Royal Holloway, University of London)

1002   Lee, J. R., 2009. Patterns of preglacial sedimentation and glaciotectonic deformation within

1003   early Middle Pleistocene sediments at Sidestrand, north Norfolk, UK. Proceedings of

1004   the Geologists' Association 120, 34-48.

1005   Lee, J. R., and Phillips, E. R. 2008. Progressive soft sediment deformation within a

1006   subglacial shear zone—a hybrid mosaic–pervasive deformation model for Middle

1007   Pleistocene glaciotectonised sediments from eastern England. *Quaternary Science*

1008   *Reviews*, *27*(13), 1350-1362

1009   Lee, J.R., Phillips, E., Booth, S.J., Rose, J., Jordan, H.M., Pawley, S.M., Warren, M.,

1010   Lawley, R.S., 2013. A polyphase glacitectonic model for ice-marginal retreat and

1011   terminal moraine development: the Middle Pleistocene British Ice Sheet, northern

1012   Norfolk, UK. Proceedings of the Geologists' Association 124, 753-777.

1013   Lee, J.R., Wakefield, O.J.W., Phillips, E., Hughes, L., 2015. Sedimentary and structural

1014   evolution of a relict subglacial to subaerial drainage system and its hydrogeological

1015   implications: an example from Anglesey, north Wales, UK. Quaternary Science

1016   Reviews 109, 88-110.

1017   Lee, J.R., Phillips, E., Rose, J., and Vaughan-Hirsch, D. 2017. The Middle Pleistocene

1018   glacial evolution of northern East Anglia, UK: a dynamic tectonostratigraphic-

1019   parasequence approach. *Journal of Quaternary Science*, *32(2),* 231-260

1020   Livingstone, S. J., Evans, D. J., Ó Cofaigh, C., Davies, B. J., Merritt, J. W., Huddart, D.,

1021   Mitchell, W. A., Roberts, D. H., and Yorke, L. 2012. Glaciodynamics of the central

1022   sector of the last British–Irish Ice Sheet in Northern England. *Earth-Science*

1023   *Reviews*, *111*(1), 25-55

1024   Livingstone, S.J., Roberts, D.H., Davies, B.J., Evans, D.J.A., Ó Cofaigh, C, and Gheorghiu,

1025   D.M. 2015. Late Devensian deglaciation of the Tyne Gap Palaeo-Ice Stream,

1026   northern England. *Journal of Quaternary Science, 30(8),* 790-804

1027

1028   Lovell, H., Livingstone, S. J., Boston, C. M., Booth, A. D., Storrar, R. D., and Barr, I. D.

1029   (2019). Complex kame belt morphology, stratigraphy and architecture. *Earth*

1030   *Surface Processes and Landforms*

1031   Macklin, M. G. 1998. The Quaternary of the Eastern Yorkshire Dales: Field gudie; the

1032   Holocene alluvial record. Quaternary Research association

1033   Madgett, P. A. 1975. Re-interpretation of Devensian Till stratigraphy of eastern

1034   England. *Nature*, *253*(5487), 105

1035   Madgett, P. A., and Catt, J. A. 1978. Petrography, stratigraphy and weathering of Late

1036   Pleistocene tills in East Yorkshire, Lincolnshire and north Norfolk. In *Proceedings*

1037   *of the Yorkshire Geological and Polytechnic Society 42(1),* 55-108. Geological

1038   Society of London

1039   Maizels, J. 1995. Sediments and landforms of modern proglacial ter- restrial environments.

1040   In Menzies, J. (ed.): *Modern Glacial Environments: Processes, Dynamics and*

1041   *Sediments,* 365–416. Butterworth-Heinemann, Oxford

1042   Maltman, A.J., 1994. *The Geological Deformation of Sediments*. Chapman and Hall,

1043   London.

1044 McMillan, A. A., and Merritt, J. W. 2012. A new Quaternary and Neogene

1045   lithostratigraphical framework for Great Britain and the Isle of Man. *Proceedings of*

1046   *the Geologists' Association*, *123*(5), 679-691

1047 Merritt, J.W., Connell, E.R. and Hall, A.M. 2017. Middle to Late Devensian glaciation of

1048   north-east Scotland: implications for the north-eastern quadrant of the last British–

1049   Irish ice sheet. *Journal of Quaternary Science*, *32*(2), 276-294

1050 Mertens, J., Vandenberghe, N., Wouters, L. and Sintubin, M. 2003. The origin and

1051   development of joints in the Boom Clay Formation (Rupelian) in Belgium. In: Van

1052   Rensbergen, P., Hillis, R.R., Maltman, A.J. and Chorley, C.K. (Eds.).,

1053   *Subsurface Sediment Mobilization*. Geological Society Special Publications 217,

1054   London, pp. 311-323.

1055 Miall, A. D. 1977. Lithofacies types and vertical profile models in braided river deposits: a

1056   summary. *Earth Science Reviews, 13,* 1-62

1057 Pawley, S. M., Bailey, R. M., Rose, J., Moorlock, B. S., Hamblin, R. J., Booth, S. J., and

1058   Lee, J. R. 2008. Age limits on Middle Pleistocene glacial sediments from OSL

1059   dating, north Norfolk, UK. *Quaternary Science Reviews*, *27*(13), 1363-1377

1060 Penny, L.F., Coope, G.R. and Catt, J.A. 1969. Age and insect fauna of the Dimlington Silts,

1061   East Yorkshire. *Nature*, *224*(5214), 65

1062 Phillips, E., Cotterill, C., Johnson, K., Crombie, K., James, L., Carr, S., and Ruiter, A. 2018.

1063   Large-scale glacitectonic deformation in response to active ice sheet retreat across

1064   Dogger Bank (southern central North Sea) during the Last Glacial

1065   Maximum. *Quaternary Science Reviews*, *179*, 24-47

1066 Piotrowski, J. A., and Kraus, A. M. 1997. Response of sediment to ice-sheet loading in

1067   northwestern Germany: effective stresses and glacier-bed stability. *Journal of*

1068   *Glaciology*, *43*(145), 489-502

1069   Piotrowski, J. A., and Tulaczyk, S. 1999. Subglacial conditions under the last ice sheet in

1070   northwest Germany: ice-bed separation and enhanced basal sliding?. *Quaternary*

1071   *Science Reviews*, *18*(6), 737-751

1072   Piotrowski, J. A., Larsen, N. K., and Junge, F. W. 2004. Reflections on soft subglacial beds

1073   as a mosaic of deforming and stable spots. *Quaternary Science Reviews*, *23*(9), 993-

1074   1000

1075   Radge, G. W. 1939. The glaciation of north Cleveland. In *Proceedings of the Yorkshire*

1076   *Geological and Polytechnic Society* 24(3), 180-205. Geological Society of London

1077   Reid, C. 1885. *The geology of Holderness, and the adjoining parts of Yorkshire and*

1078   *Lincolnshire* (Vol. 47). HM Stationery Office.

1079   Reimann, C., Filzmoser, P., Garrett, R. G., and Dutter, R. 2008. Statistical data analysis

1080   explained. *Applied environmental statistics with R. England: Wiley & Sons Ltd*

1081   Richards, A. E. 1998. Re-evaluation of the Middle Pleistocene stratigraphy of

1082   Herefordshire, England. *Journal of Quaternary Science*, *13*(2), 115-136

1083   Roberts, D. H., and Hart, J. K. 2005. The deforming bed characteristics of a stratified till

1084   assemblage in north East Anglia, UK: investigating controls on sediment rheology

1085   and strain signatures. *Quaternary Science Reviews*, *24*(1), 123-140

1086   Roberts, D. H., Evans, D. J. A., Lodwick, J. and Cox, N. J. 2013. The subglacial and ice-

1087   marginal signature of the North Sea Lobe of the British-Irish Ice Sheet during the

1088   Last Glacial Maximumat Upgang, North Yorkshire, UK. *Proceedings of the*

1089   *Geologists' Association, 124*, 503–519

1090   Roberts, D. H., Evans, D. J., Callard, S. L., Clark, C. D., Bateman, M. D., Medialdea, A.,

1091   Dove, D., Coterill, C. J., Saher, M., Ó Cofaigh, C., Chiverrell, R. C. Moreton, S. G.,

1092   Fabel., D., and Bradwell. T. 2018. Ice marginal dynamics of the last British-Irish Ice

1093   Sheet in the southern North Sea: Ice limits, timing and the influence of the Dogger

1094   Bank. *Quaternary Science Reviews*, *198*, 181-207

1095 Roberts, D. H., Grimoldi, E., Callard, L., Evans, D. J., Clark, C. D., Stewart, H. A., and

1096   Bateman, M. D. 2019. The mixed-bed glacial landform imprint of the North Sea

1097   Lobe in the western North Sea. *Earth Surface Processes and Landforms*, *44*(6),

1098   1233-1258

1099 Robson, D.A., 1976. "A guide to the geology of the Cheviot Hills". *Transactions of the*

1100   *Natural History Society of Northumbria,* 43(1), pp. 23

1101 Rose, J. 1985. The Dimlington Stadial/Dimlington Chronozone: a proposal for naming the

1102   main glacial episode of the Late Devensian in Britain. *Boreas*, *14*(3), 225-230

1103 Small, D., Clark, C.D., Chiverrell, R.C., Smedley, R.K., Bateman, M.D., Duller, G.A., Ely,

1104   J.C., Fabel, D., Medialdea, A. and Moreton, S.G. 2017. Devising quality assurance

1105   procedures for assessment of legacy geochronological data relating to deglaciation of

1106   the last British-Irish Ice Sheet. *Earth-Science Reviews*, *164*; 232-250

1107 Scourse, J.D., Ward, S.L., Wainwright, A., Bradley, S.L. and Uehara, K. 2018. The role of

1108   megatides and relative sea level in controlling the deglaciation of the British–Irish

1109   and Fennoscandian ice sheets. *Journal of Quaternary Science*, *33*(2); 139-149

1110 Scheib, A. J., Lee, J. R., Breward, N., and Riding, J. B. 2011. Reconstructing flow paths of

1111   the Middle Pleistocene British Ice Sheet in central-eastern England: the application

1112   of regional soil geochemical data. *Proceedings of the Geologists'*

1113   *Association*, *122*(3), 432-444

1114 Scourse, J. D., Haapaniemi, A. I., Colmenero-Hidalgo, E., Peck, V. L., Hall, I. R., Austin,

1115   W. E., Knutz, P. C., and Zahn, R. 2009. Growth, dynamics and deglaciation of the

1116   last British–Irish ice sheet: the deep-sea ice-rafted detritus record. *Quaternary*

1117   *Science Reviews*, *28*(27), 3066-3084

1118   Smith, D.B., 1995. "Permian and Triassic". In Johnson, G.A.L., 1995 (ed.), "Robson's

1119   Geology of northeast England". *Transactions of the Natural History Society of*

1120   *Northumbria,* Volume 56, Part 5, p. 283-296

1121   Stokes, C. R., Tarasov, L., Blomdin, R., Cronin, T. M., Fisher, T. G., Gyllencreutz, R., and

1122   Jakobsson, M. 2015. On the reconstruction of palaeo-ice sheets: recent advances and

1123   future challenges. *Quaternary Science Reviews*, *125*, 15-49

1124   Stone, P, Millward, D, Young, B, Merritt, J. W., Clarke, S.M., McCormac, M., and

1125   Lawrence, D. J. D. 2010. British Regional Geology: Northern England (Firth

1126   edition). Keyworth, Nottingham: British Geological Survey, HMSO

1127   Stow, D. A. 2005. *Sedimentary rocks in the Field: a colour guide*. Gulf Professional

1128   Publishing

1129   Stroeven, A. P., Hättestrand, C., Kleman, J., Heyman, J., Fabel, D., Fredin, O., and Caffee,

1130   M. W. 2016. Deglaciation of fennoscandia. *Quaternary Science Reviews*, *147*, 91-

1131   121

1132   Taylor, B. J., and Eastwood, T. 1971. *Northern England* (Vol. 7). HM Stationery Office.

1133   Toghill, P. 2011. *The geology of Britain: an introduction*. Wiltshire, UK, Swanhill Press

1134   Trewin, N. H. 2002. *The Geology of Scotland.* Fourth Edition. London, The Geological

1135   Society of London, pp. 576

1136   van der Wateren, F. M. 1995. Structural geology and sedimentology of push moraines:

1137   processes of soft sediment deformation in a glacial environment and the distribution

1138   of glaciotectonic styles, *Mededelingen Rijks Geologische Dienst 54*

1139   Walder, J. S., and Fowler, A. 1994. Channelized subglacial drainage over a deformable

1140   bed. *Journal of Glaciology*, *40*(134), 3-15

1141   Walden, J. S. 2004. Particle Lithology (or mineral and geochemical analysis). *A practical

1142   guide to the study of glacial sediments*. In D. J. A. Evans and D. I. Benn. London,

1143   Arnold, 145-180

1144   Wood, S. V., and Rome, J. L. 1868. On the glacial and postglacial structure of Lincolnshire

1145   and south-east Yorkshire. *Quarterly Journal of the Geological Society*, *24*(1-2), 146-

1146   184

1147   **FIGURE CAPTIONS**
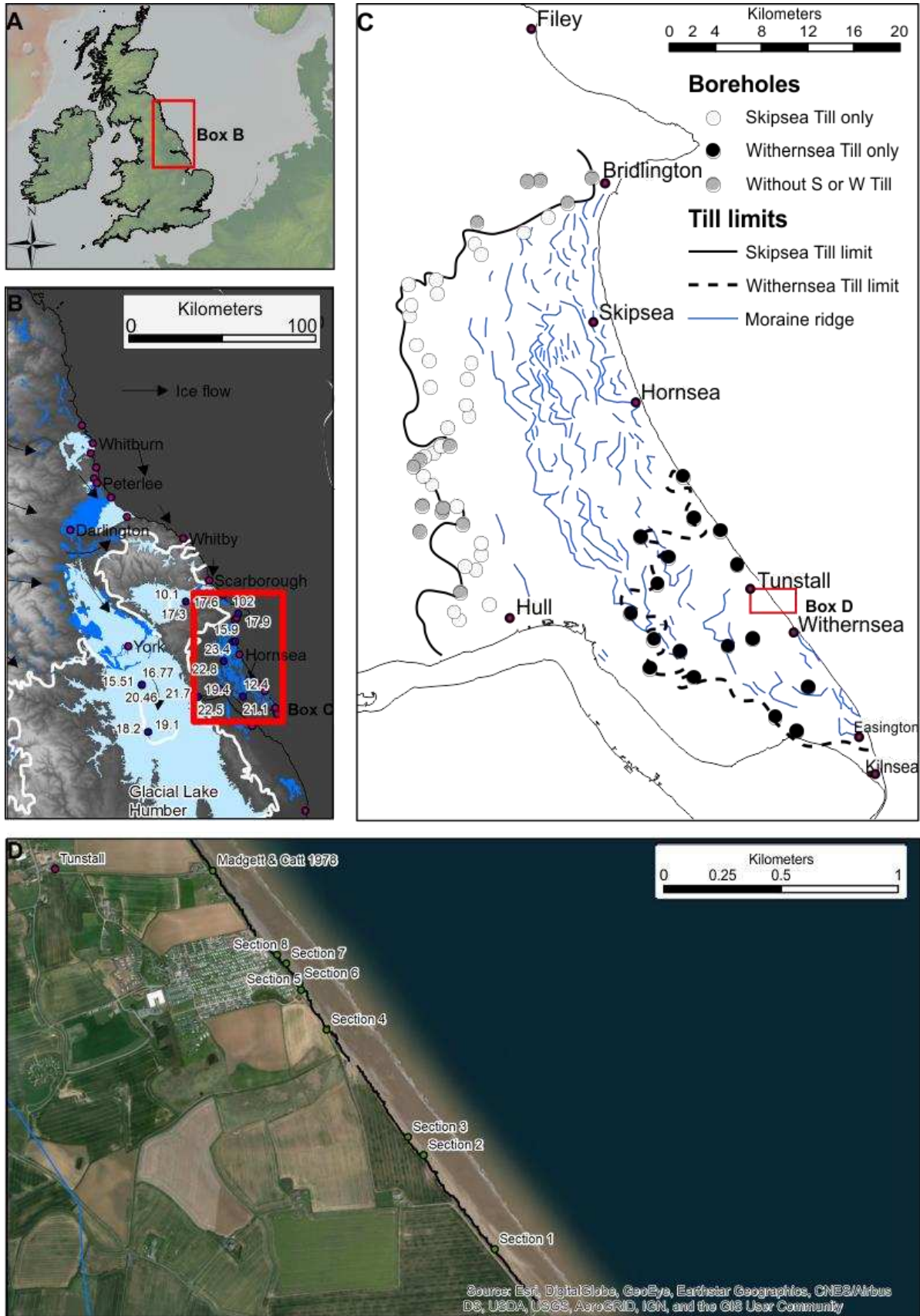
Figure 1. **A.** Great Britain and study area highlighted. **B.** The Yorkshire and Durham
coastline, with places named in the text. **C.** Study area, showing limits of Skipsea and
Withernsea Tills (from Evans and Thomson, 2010). Published ages and geomorphology

1152   from Clark *et al*. (2018); Bateman *et al*. (2015; 2017); Evans *et al*. (2016). **D.** Detail of
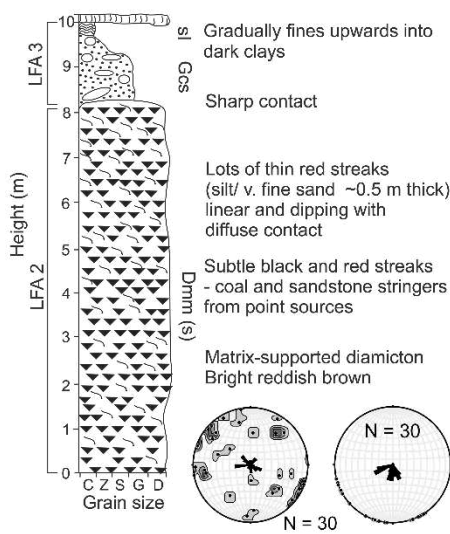1153   study area, showing location of section logs. Imagery from ArcMap Basemap

1154

1155
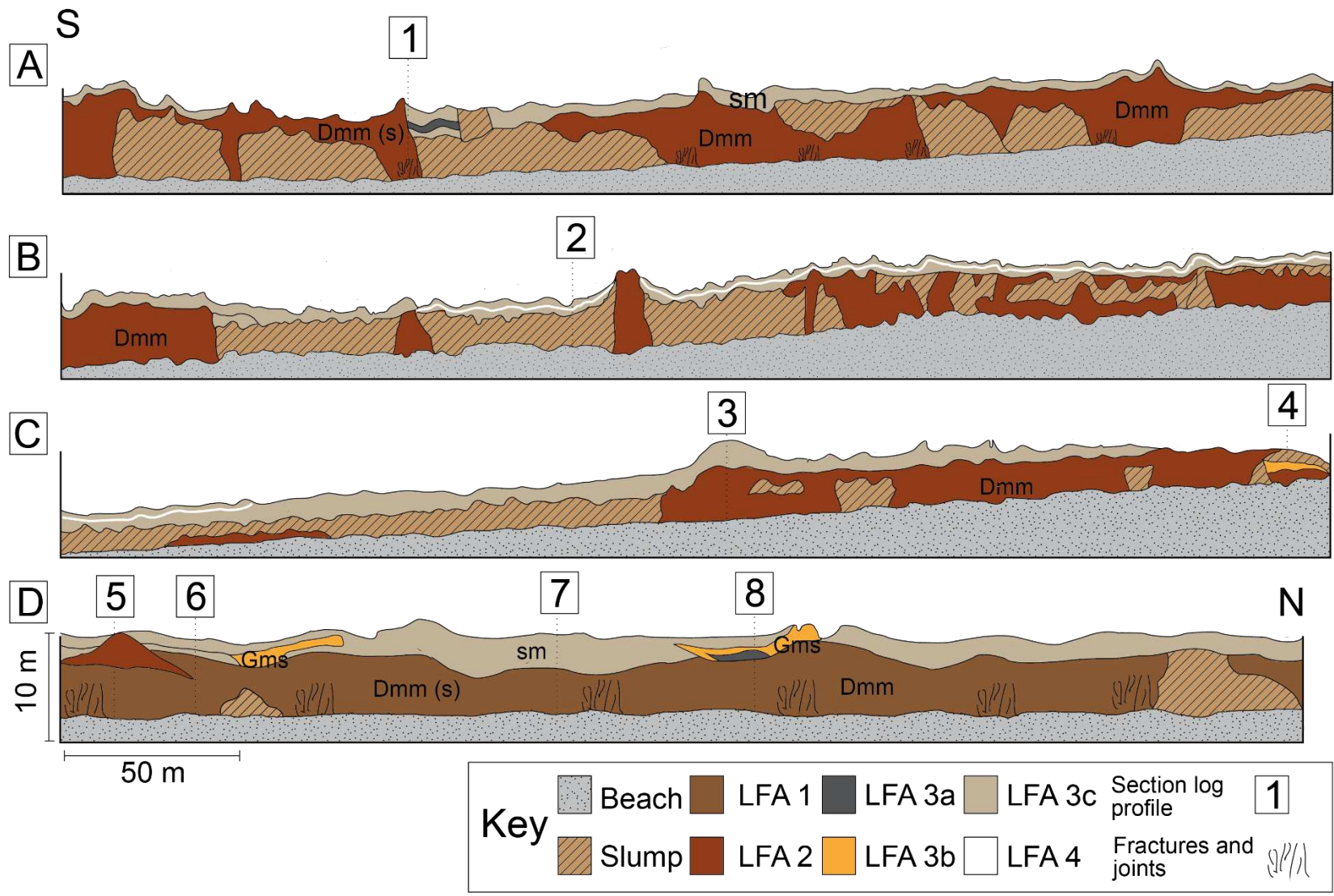
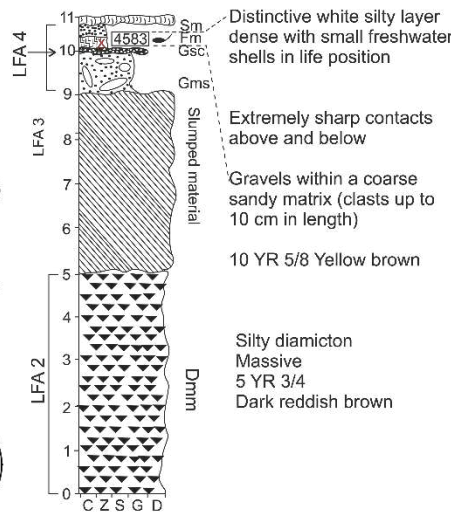**Figure 2.** Facies architecture with clast fabric and straie orientation at Tunstall

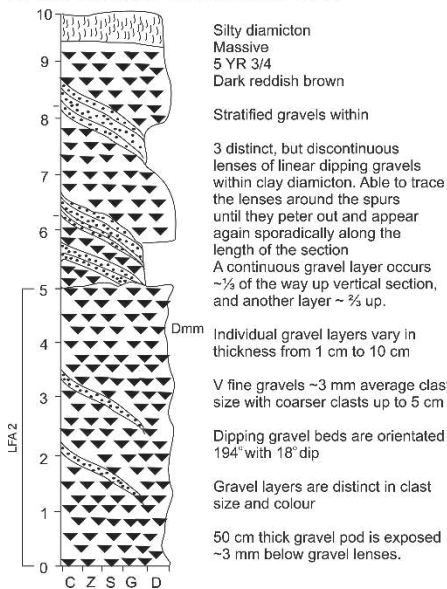**Section log no. 1**

GPS co-ordinates : TA 32574 BNG 30149

LFA 3

LFA 2

Gradually fines upwards into dark clays

Sharp contact

Lots of thin red streaks (silt/ v. fine sand ~0.5 m thick) linear and dipping with diffuse contact

Subtle black and red streaks - coal and sandstone stringers from point sources

Matrix-supported diamicton Bright reddish brown

N = 30

N = 30

Section log no. 2

GPS co-ordinates : TA 32266 BNG 30557

Distinctive white silty layer dense with small freshwater shells in life position

Extremely sharp contacts above and below

Gravels within a coarse sandy matrix (clasts up to 10 cm in length)

10 YR 5/8 Yellow brown

Silty diamicton Massive 5 YR 3/4 Dark reddish brown

Section log no. 3

GPS co-ordinates : TA 31848 BNG 31109

Silty diamicton Massive 5 YR 3/4 Dark reddish brown

Stratified gravels within

3 distinct, but discontinuous lenses of linear dipping gravels within clay diamicton. Able to trace the lenses around the spurs until they peter out and appear again sporadically along the length of the section A continuous gravel layer occurs ~⅓ of the way up vertical section, and another layer ~ ⅔ up.

Individual gravel layers vary in thickness from 1 cm to 10 cm

V fine gravels ~3 mm average clast size with coarser clasts up to 5 cm

Dipping gravel beds are orientated 194° with 18° dip

Gravel layers are distinct in clast size and colour

50 cm thick gravel pod is exposed ~3 mm below gravel lenses.

Section log no. 4

GPS co-ordinates : TA 31869 BNG 31111

Spoil. Human influenced - wires and polystyrene (appears to be in situ) non-uniform Tabular bed. Dips 05" to south Dip angle changes frequently

Sharp lower contact Laterally variable Very coarse gravels, Gradually fines upwards into clast-supported sandy gravels Majority of clasts are rounded Broken clasts visible Durable lithologies only sometimes bedded, often chaotic 5 YR 4/6 Reddish Brown Base of unit follows undulating bedrock Fissile Contains non-durable and durable clasts Striated sub-angular and sub-rounded clasts Stringers from point sources (coal and sandstone)

LFA 3c

N = 50

LFA 1

N = 20

N = 50
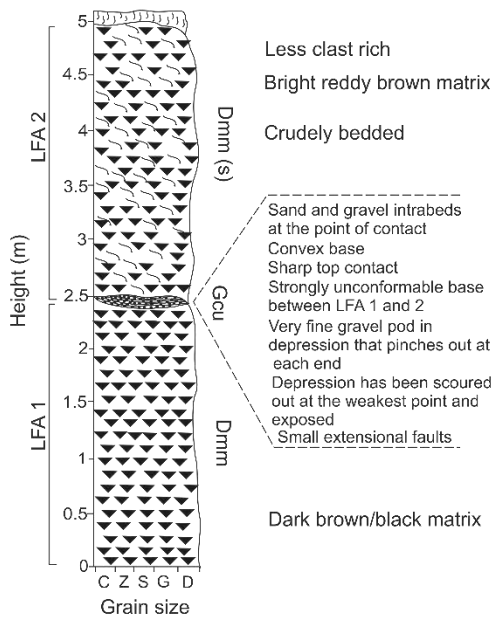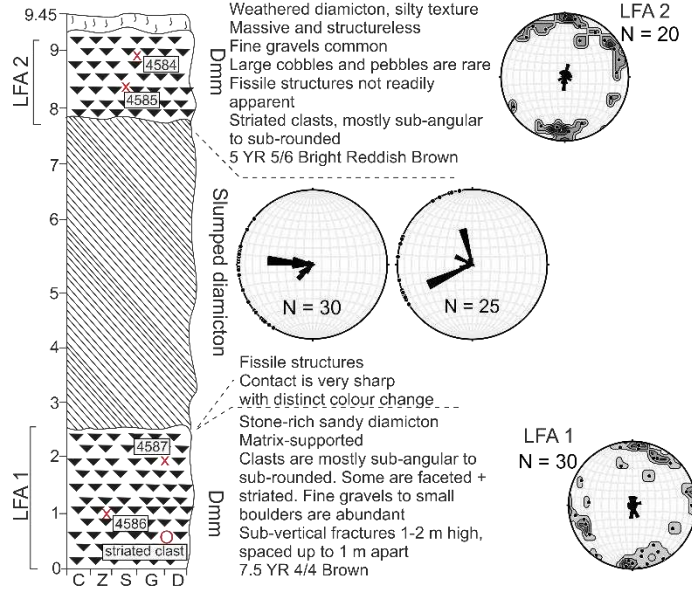
Figure 3a. Section logs 1 – 4 (see Figure 2 for log locations). Note differences in vertical scale
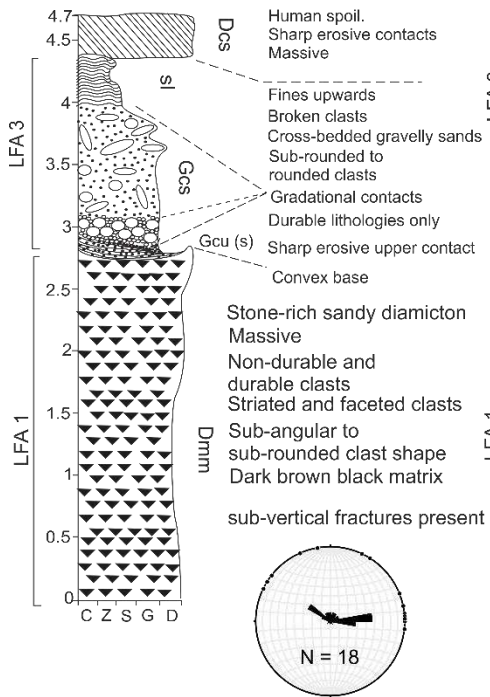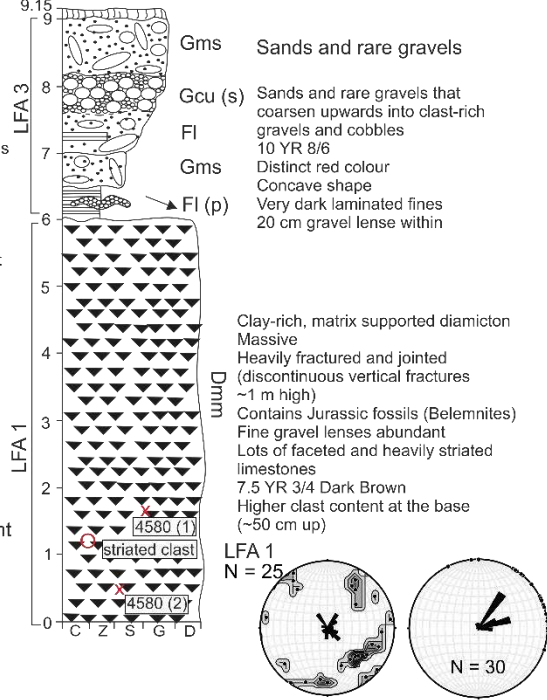
Figure 3b. Section logs 5 – 8 (see Figure 2 for log locations). Note differences in vertical scale
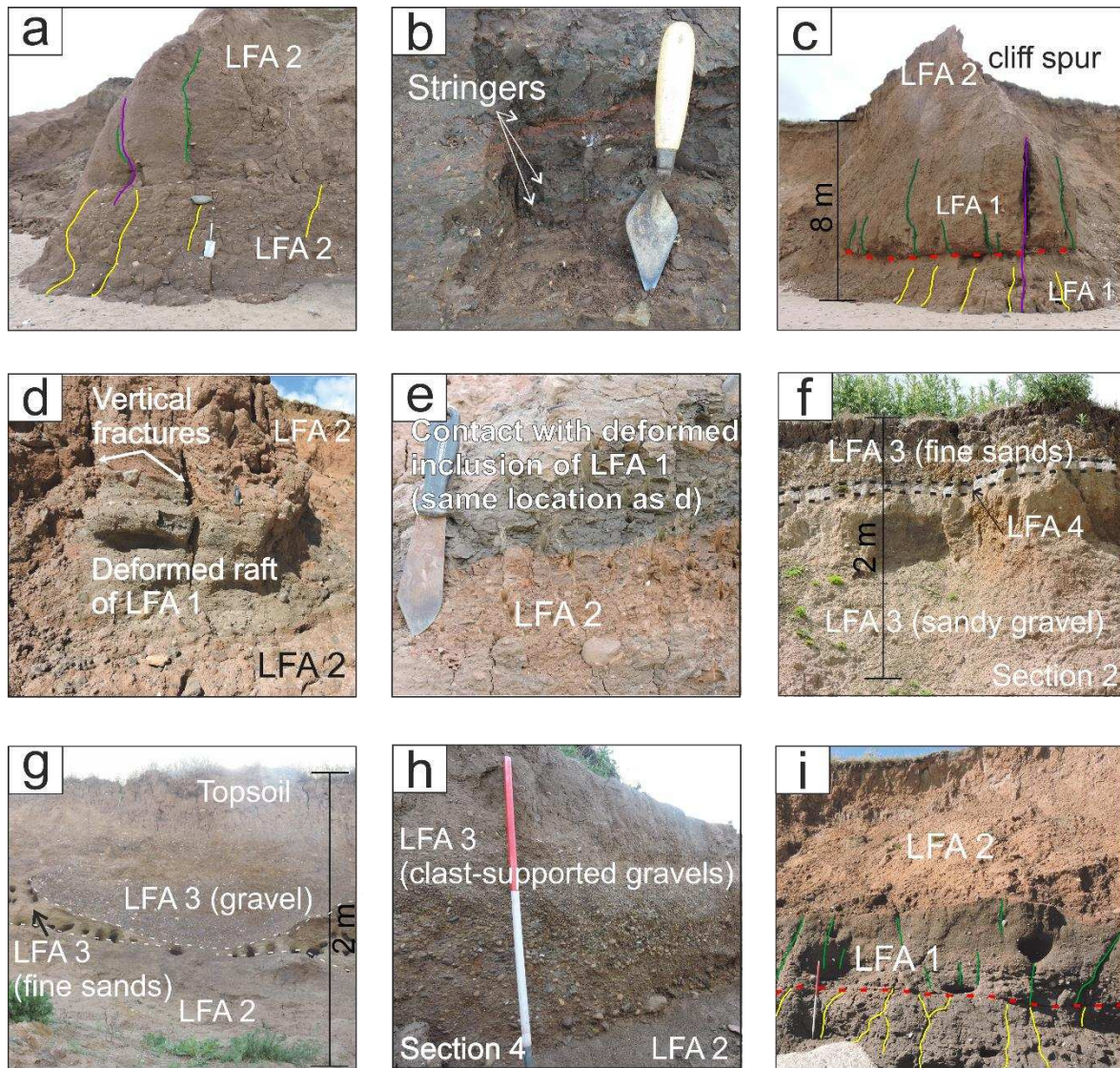
Figure 4. Representative photographs of key features at Tunstall including fracture sets F1 (yellow), F2 (red), F3 (green) and F4 (purple). **a.** LFA 1 and LFA 2 in superposition showing fracture sets **b.** Stringers of red and black diamicton up to 10 cm thick in LFA 1 **c.** Fracture sets F1, F2 and F3 in LFA 1 **d.** Raft of LFA 1 in LFA 2 **e.** Contact between LFA 2 and the deformed inclusion of LFA 1 **f.** Nature of LFA 4 **g.** Channel structure **h.** Cast-supported gravels in LFA 3 **i.** LFA 1 and 2 in superposition, showing F1 and F2 fracture sets
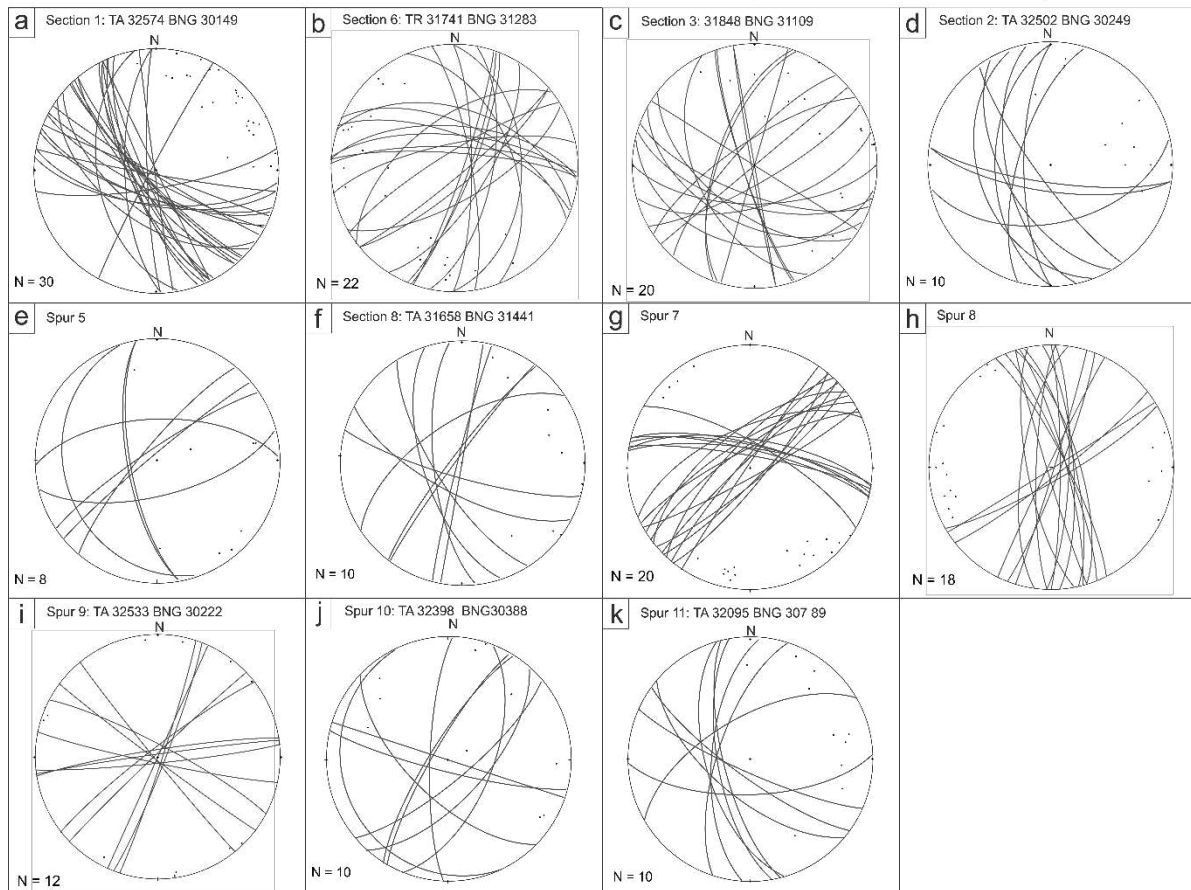
Figure 5. Fracture measurements (dip angle and dip azimuth) plotted as poles to planes and great circles on stereographic projections.
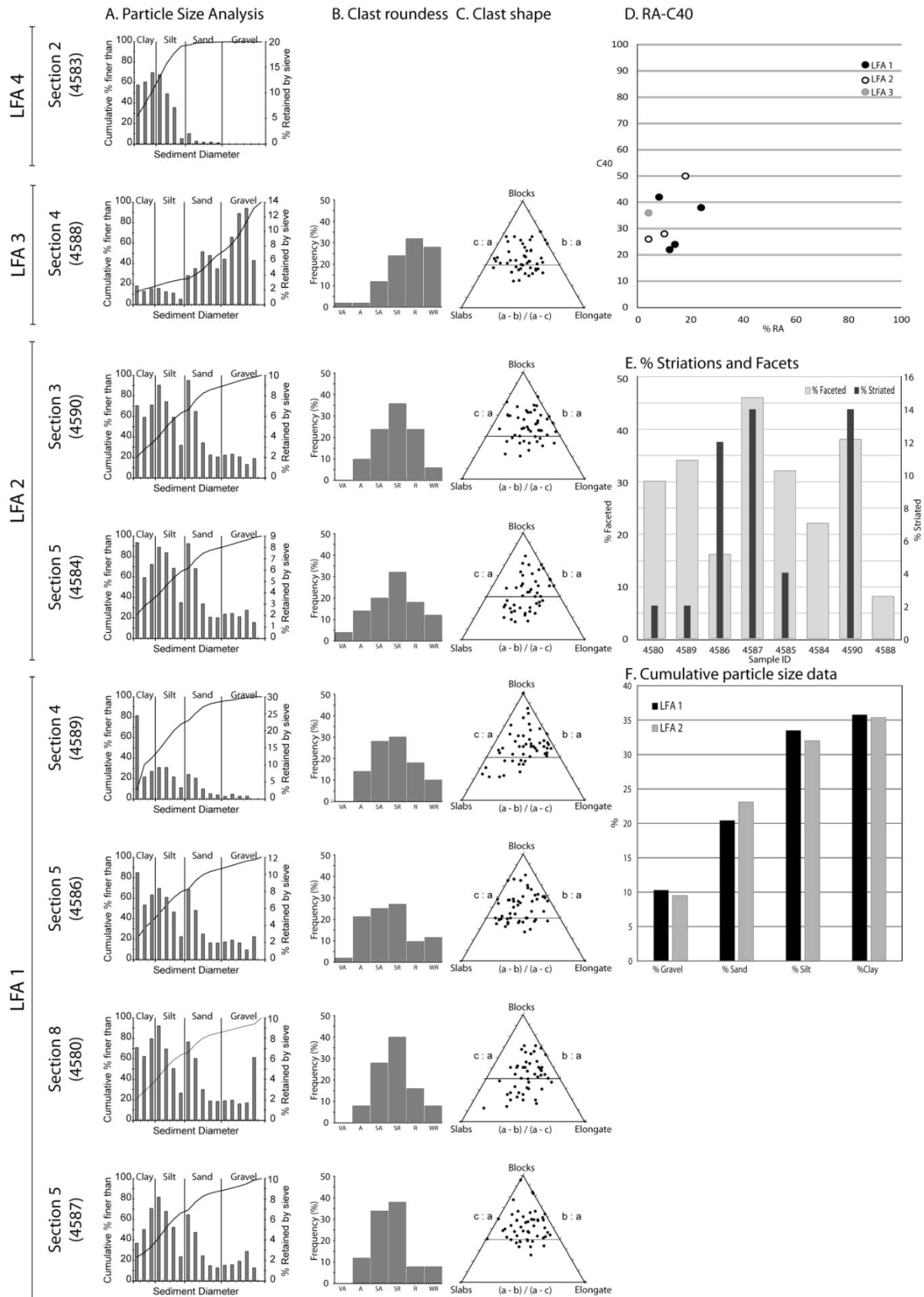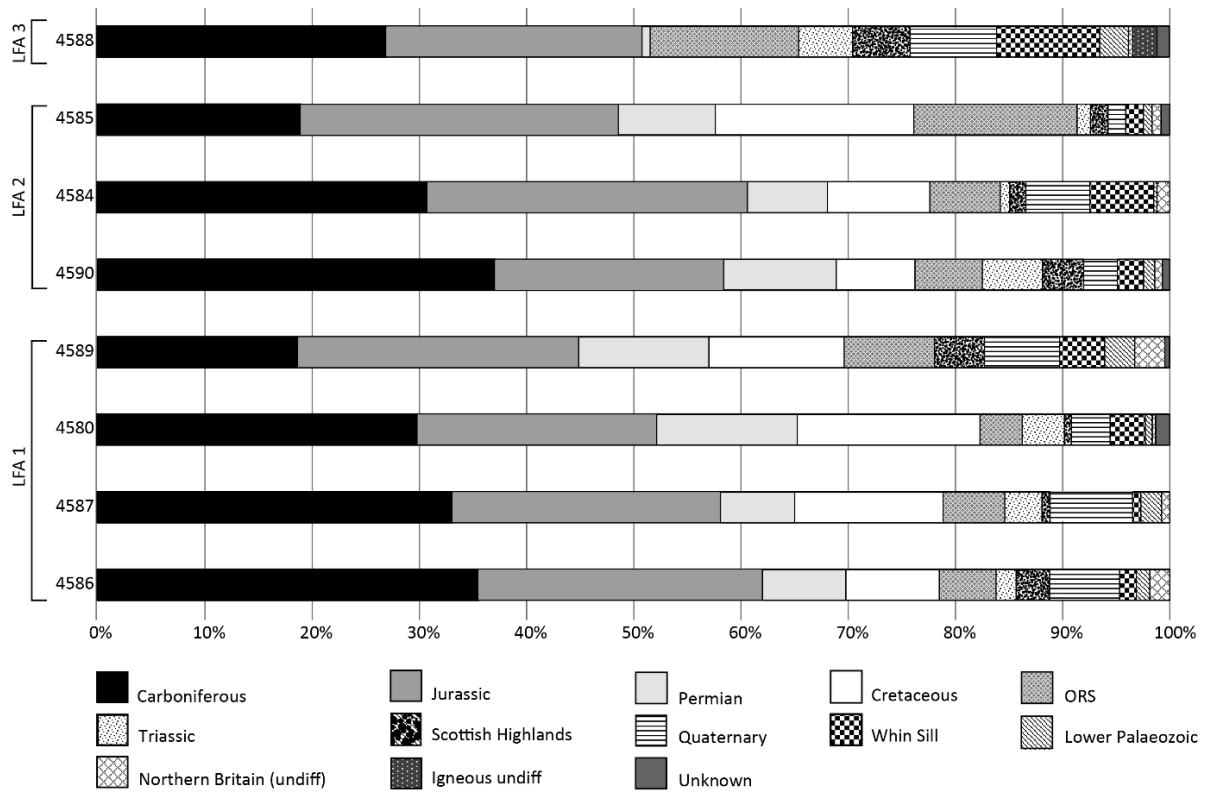
1174

Figure 6. A. Particle size distribution for each sample. **B.** Clast roundness for gravel

fraction. **C.** Clast shape for gravel fraction. **D.** RA-C40 graph. **E.** Percentage of striated and

faceted stones within the gravel fraction. **F.** Total percentages of clay, silt, sand and gravel

1178 in each lithofacies.

1179

1180 **Figure 7.** Clast lithological analysis for each sample

**Figure 8.** Representative photographs of key erratic lithologies in each sample **a.**
Greywacke (LFA 2) **b.** Whin Sill Dolerite (LFA 2) **c.** Old Red Sandstone (LFA 1) **d.**
Andesitic porphyry (LFA 2) **e.** Sherwood Sandstone (LFA 1) **f.** Magnesian Limestone (LFA
1) **g.** K-feldspar rich Granite (LFA 2) **h.** Rhyolite (LFA 3) **i.** Carboniferous Limestone (LFA
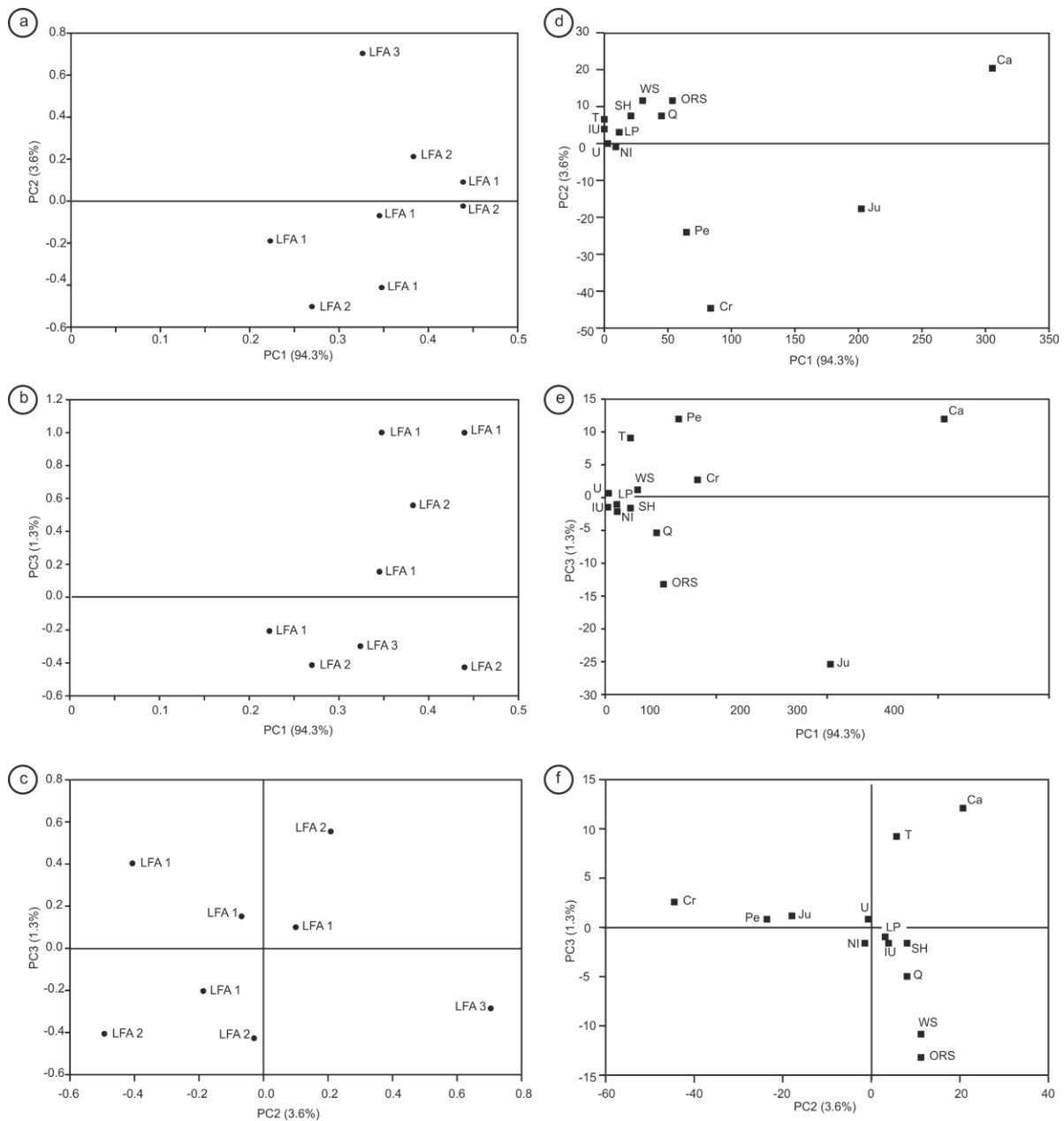1) **j.** K-feldspar <Quartz Granodiorite (LFA 1) **k**. Cheviot Granite (LFA 3) **l.** Quartzite
(LFA 1).
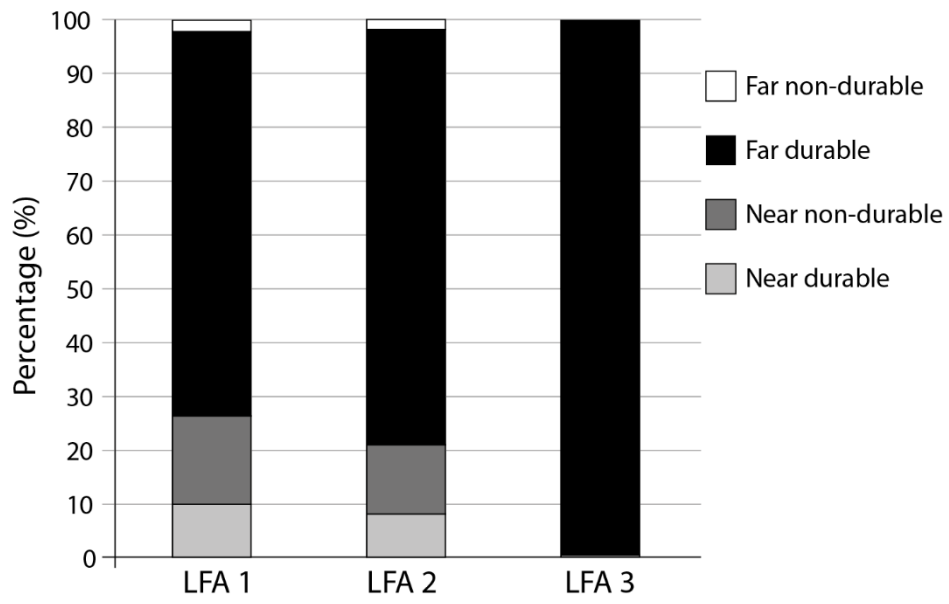
1189   **Figure 9.** Durability of far travelled and local clasts in each lithofacies

**Figure 10.** Plotting of processed PCA data. **a.** Principal component scores PC 1 and PC 2 **b.** Principal component scores PC 1 and PC 3 **c.** Principal component scores PC 2 and PC 3 **d.** Principal Component coefficients displaying lithological relationships between PC1 and PC2 **e.** Principal Component coefficients displaying lithological relationships between PC1 and PC3 **f.** Principal Component coefficients displaying lithological relationships between PC2 and PC3
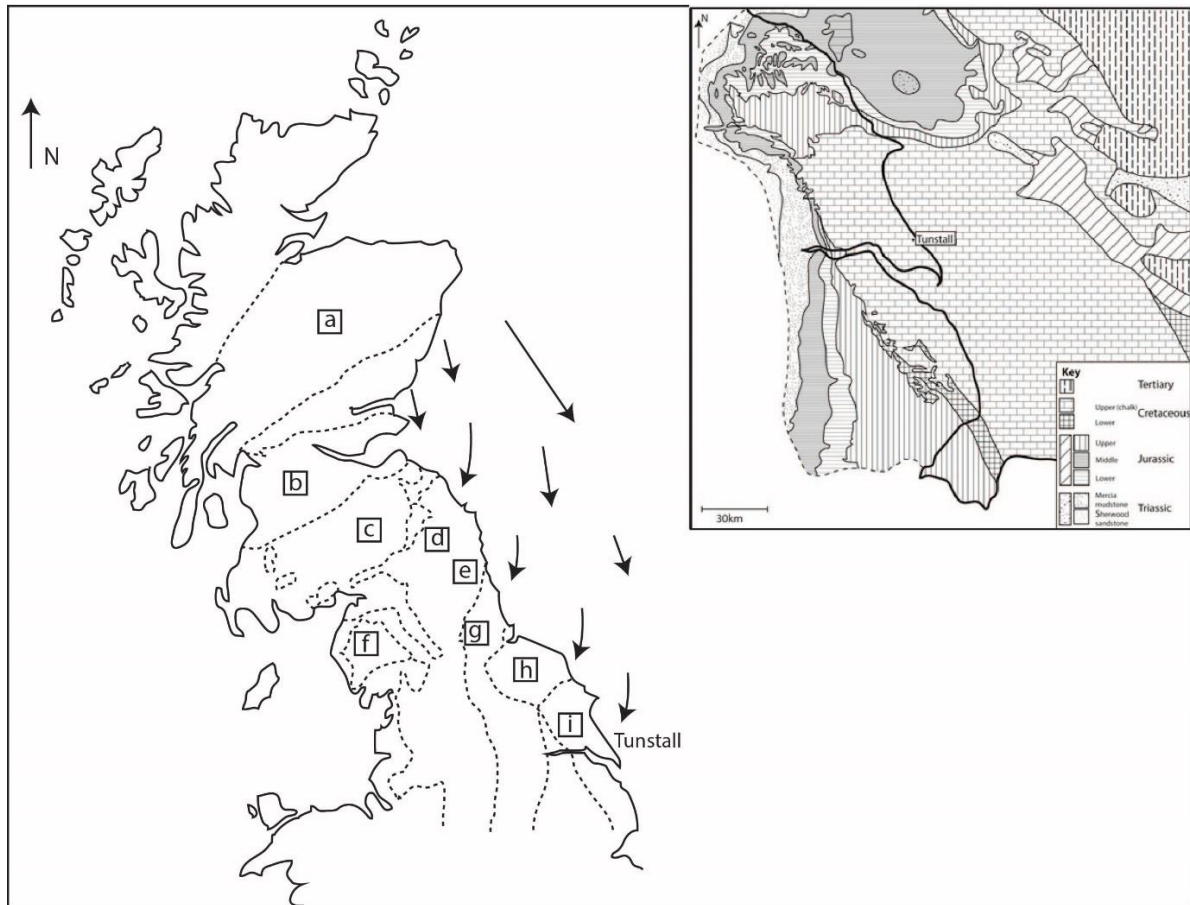
Figure 11. Revised iceflow pathways inferred from the simplified bedrock geology map of
Northern Britain with outcrop occurances of the lithostratigraphical group .a. Grampian
Highlands b. Midland Valley c. southern uplands d. Cheviot volcanic complex e.
Northumberland f. Lake District volcanic complex g. County Durham h. Cleveland basin i.
Yorkshire basin Insert – Detailed map of the solid geology from the Tees estuary to The
Wash (adapted from Kent and Gaunt, 1980; Busfield *et al*., 2015).

TABLE CAPTIONS

	LFA 1	LFA 2	LFA 3	LFA 4
% Gravel	10.29	9.5	47.07	0.00
% Sand	20.41	23.1	27.74	3.22
% Silt	33.47	32	8.44	45.29
% Clay	35.78	35.4	16.75	51.49

1205   **Table 1.** Particle size analysis for each lithofacies at Tunstall

1206

1207

	Clast Lithology	LFA 1	LFA 2	LFA 3
Total (n)		**893**	**847**	**260**
Carboniferous	Arkose sandstone	2.46	4.57	0.00
	Carboniferous sandstone	13.66	18.44	26.54
	Carboniferous Chert	0.00	0.16	0.00
	Carboniferous Mudstone	0.00	0.16	0.00
	Carboniferous Limestone	9.52	7.38	0.00
	Coal	2.13	1.44	0.00
	Limestone undiff	3.81	0.64	0.00
	Basaltic Porphyry	0.56	0.96	0.38
	Carboniferous Porphyry	0.45	0.00	0.00
Permian	Sherwood Sandstone	2.69	3.05	0.77
	Magnesian Limestone	6.61	5.77	0.00
Triassic	Mercia Mudstone	3.02	3.05	0.00
	Red Siltstone	0.00	0.00	5.00
Jurassic	Jurassic Sandstone	6.16	7.54	3.08
	Yellow Sandstone	1.34	1.28	5.38
	Quartzitic Sandstone	1.12	0.96	0.00
	Siltstone undiff	4.03	6.26	8.46
	Yellow Siltstone	0.22	0.16	0.00
	Jurassic Mudstone	11.65	6.98	6.54
	Ironstone	0.00	0.80	0.38
	Jurassic Limestone	0.56	1.76	0.00
	Oolitic Limestone	0.00	0.16	0.00
Cretaceous	Cretaceous Chert	0.00	0.16	0.00
	Chert undiff	2.58	1.92	0.00
	Chalk	10.41	6.58	0.00
	Flint	0.22	0.32	1.54
Quaternary	Silcrete	0.00	0.16	0.00
	Brown Quartzite/ Vein Quartz	3.25	2.41	4.23
	Red Quartzite/ Vein Quartz	0.56	0.48	0.00
	White Quartzite/Vein Quartz	1.79	1.28	2.31
Lower Palaeozoic	Greywacke	1.23	0.48	2.69
Northern Britain	Gabbro	0.00	0.32	0.38
	Basalt	1.01	0.64	0.00
Whin Sill	Whin Sill Dolerite	1.90	4.33	9.62
Old Red Sandstone	Old Red Sandstone	2.91	2.25	6.15
	Old Red Sandstone porphyry	0.34	0.48	0.00
Scottish Highlands	Diorite	0.78	0.32	1.92
	Grano-diorite	0.22	0.16	0.00
	Micro-granite	0.00	1.12	3.08
	Granite	0.00	0.00	0.38
	Schist	0.45	0.48	0.00
	Phyllite	0.22	0.32	0.00
	Gneiss	0.00	0.08	0.00
Igneous	Igneous undiff	0.00	0.00	2.31
	Rhyolite	0.45	1.12	1.15
	Andesite	0.56	0.96	1.54
	Felsite	0.00	0.32	0.00
	Andesitic Porphyry	0.45	0.64	1.54
	Rhyolitic Porphyry	0.22	0.80	3.46
Unknown		0.45	0.32	1.15

1209   **Table 2.** Clast lithological data, showing percentages of clasts in each lithofacies

1210

Event/Stage	Description	Interpretation	Implication
I	Massive, matrix-supported diamicton	Deposition of subglacial traction till (LFA 1; lower Skipsea Till)	Initial advance from NSL
II	Sub-vertical fractures (upwards to F2)	Unloading and shrinkage; development of F1 fractures	Sub-aerial exposure of ice-marginal retreat or thinning
Hiatus (Short)			
IV	Massive-matrix-supported diamicton	Thrust-stacking of LFA 1 (derived from nearby but up-ice) ontop of LFA 1 (decollement surface eventually became F2)	Re-advance of NSL
V	Sub-horizontal fracturing along pre-exiting plane of weakness (décollement developed in stage iv)	Unloading and development of F2 fractures	Retreat of the NSL
VI	Massive, matrix-supported diamicton	Subglacial emplacement of LFA 2	Re-advance of NSL
VII	Sub-vertical fractures (upwards from F2)	Unloading and shrinkage; development of F3 fractures	Subaerial exposure of ice-marginal retreat or thinning
VIII	Sands and gravels	Deposition of LFA 3; proximal glaciofluvial outwash	Retreat following advance but no overriding of site; final stages of deglaciation
IX	White organic silt	Deposition of LFA 4 (Tufa)	Spring-fed pool under temperate icefree conditions

X	Sub-vertical fractures (F4)	Lateral release joints	Coastal erosion

1211 **Table 3.** Summary of litho-tectonic event stratigraphy described from the base (oldest) to

1212 the top (youngest) in superpositional order

SUPPLEMENTARY INFORMATION

Code	Description
Diamictons	
Dmm	Matrix-supported, massive
Dcs	Clast-supported, massive
---(s)	Stratified
Gravels	
Gms	Matrix-supported, massive
Gcs	Clast-supported
Gcu	Upwards coarsening gravels (inverse grading)
---(s)	Stratified
Sands	
Sm	Massive
Sl	Horizontal and draped lamination
Silts and Clays	
Fm	Massive
Fl	Fine lamination (minor sand and very small

ripples

---(p)	Intraclast or lens

SUPPLEMENTARY Table A1. Lithofacies codes used in this study (and those in **Figure**

3a, **b**), adapted from Benn and Evans (1998)